AD-A040 900 GEO-CENTERS INC NEWTON UPPER FALLS MASS F/G 17/9
THE APPLICATION OF PATTERN RECOGNITION TECHNIQUES FOR TUNNEL LO--ETC(U)
NOV 76 DAAG53-76-C-0180
UNCLASSIFIED GC-TR-76-1009 NL

1 OF 1
ADA040900

END

DATE
FILMED
7-77

GC-TR-76-1009

AD A040900

THE APPLICATION OF PATTERN RECOGNITION TECHNIQUES FOR TUNNEL LOCATION

Contract No. DAAG-53-76-C-0180

GEO-CENTERS, INC.
381 Elliot Street
Newton Upper Falls, MA 02164

November 30, 1976

GEO-CENTERS, INC.

Table of Contents

Figures

Figures

Figures

I. Introduction

The location of buried tunnels is part of an ongoing program at DARPA with many different disciplines and techniques involved in the effort. Geo-Centers, Inc. effort to locate buried tunnels was originally funded by DARPA for a period of five months beginning in June 1976. The major thrust of that effort was the theoretical investigation of special computer assisted detection methods to locate tunnels. The basic electromagnetic signal was theoretically generated using the principles of video pulse radar. This radar technique uses a short time limited electromagnetic pulse radiated by a movable antenna platform at the earth-air interface. The objectives of the original tunnel detection study were successfully realized; namely, the development of a rapid and sensitive signal processing technique which was tested using a number of realistic models.

The major emphasis of the Geo-Centers' program was the development of a signal processing method to detect buried tunnels using video pulse radar probes. Video pulse radar is used to transmit and receive a short unidirectional electromagnetic pulse. The return pulse in turn produces a two dimensional sounding or picture. Theoretical soundings were generated based on a simple scattering model relevant to long cylindrical tunnels that are buried in granite. A fast and sensitive picture processing algorithm was evolved for the specific problem

of subsurface tunnel detection. The utility of the algorithm has been tested in a variety of situations including: (1) multiple tunnels, (2) large noise or clutter background values, and (3) interfering or blocking layers. In all cases the detection algorithm is unusually stable and dependable. The present method requires a human operator for final recognition.

The basic theory for generating the subsurface soundings is related to the "geometrical optics" approach of diffraction theory. The transmission and reflection coefficients at the tunnel walls are given approximately by the plane wave values. Geometrical ray paths are used to compute the time for each tunnel return. This method of generating subsurface soundings is quite adequate except in the lower frequency range of the incident pulse. However, it is the high frequency part of the pulse that is concerned with resolving tunnel location.

The basic tunnel detection scheme involves the application of a new concept in signal detection. In this scheme, a "geometrical filter" has been used to detect the special tunnel returns that are found on the two dimensional soundings. The actual method used to construct the filter is based on real space reconstruction methods used to generate three dimensional pictures from a series of two-dimensional projections. One-dimensional projections are used to reconstruct the sounding. They are chosen so as to give superior tunnel representations. The reconstruction algorithms act as a shape sensitive filter

to emphasize only the tunnel attributes of the soundings and are insensitive to other objects and clutter on the original sounding. Once the soundings have been processed by the "geometrical filter," the tunnel locations are clearly evident to the observer.

A. The Application of Pattern Recognition Techniques for Tunnel Location*

In our recent study, representative subsurface soundings were generated using a modified geometrical optics method for scattering by dielectric bodies.[1] The basic building block used in this theory is the time domain pulse reflected from a semi-infinite medium. Pulses scattered from a cylinder are decomposed into a superposition of reflections from the surfaces of a buried cylinder used to model the tunnel. Geometrical paths were used to compute the times for the individual reflections. Steady state transfer functions were superimposed through the Fourier integral to produce the time domain signals. A sample steady state transfer function is shown in Figure 1 and a pulse reflected from a tunnel buried in granite is given in Figure 2. A Gaussian incident pulse of specified half-width is assumed to be propagated into the earth at ground zero. Values of the electrical parameters were: conductivity $\sigma = 10^{-3}$ and 10^{-4}, and relative dielectric constant $\varepsilon_r = 7$. A two dimensional sounding formed by moving a probing antenna over

---

* Material presented in this section is considered proprietary by DARPA and Geo-Centers, Inc.

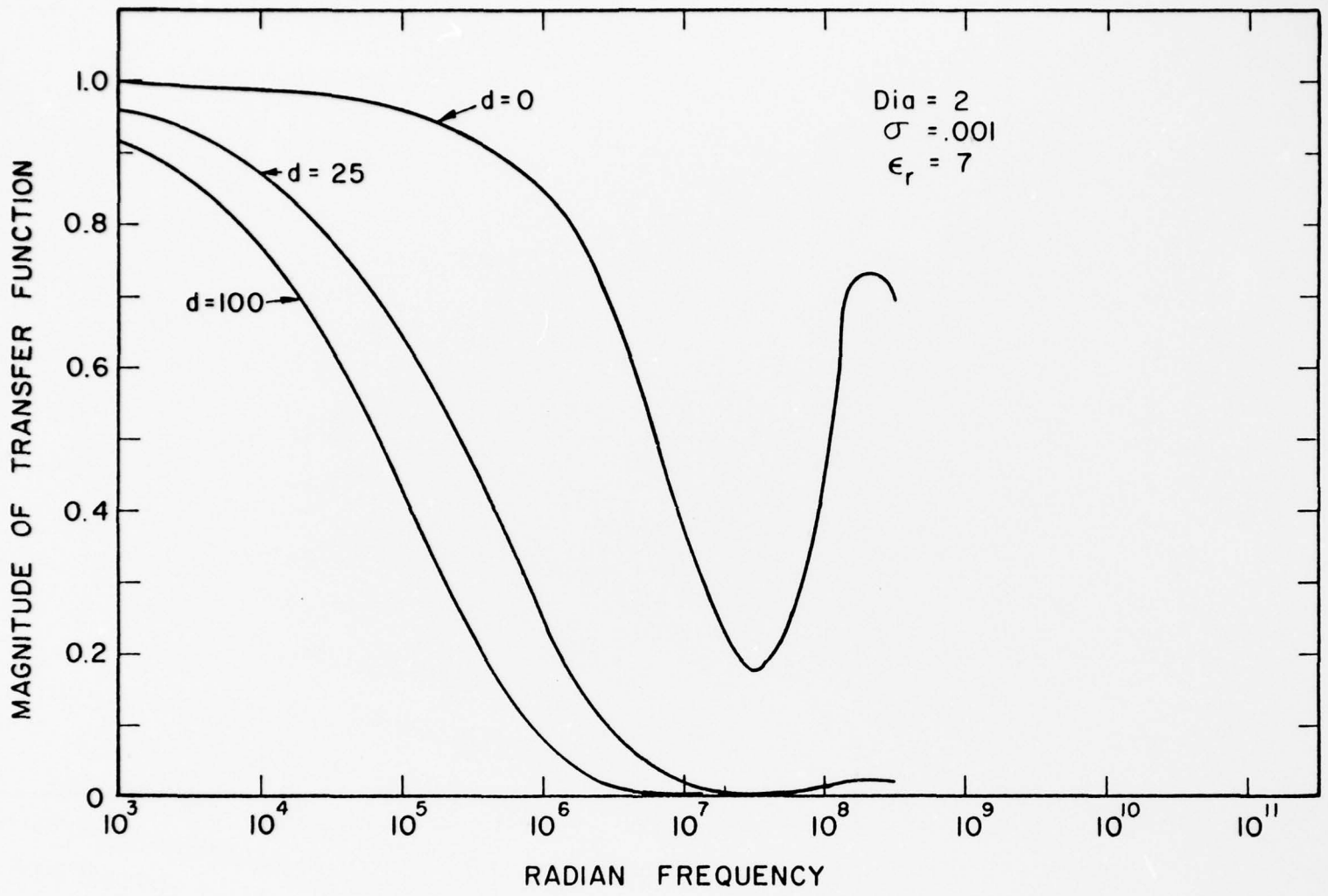

FIGURE 1 TRANSFER FUNCTION FOR REFLECTIONS FROM A BURIED TUNNEL

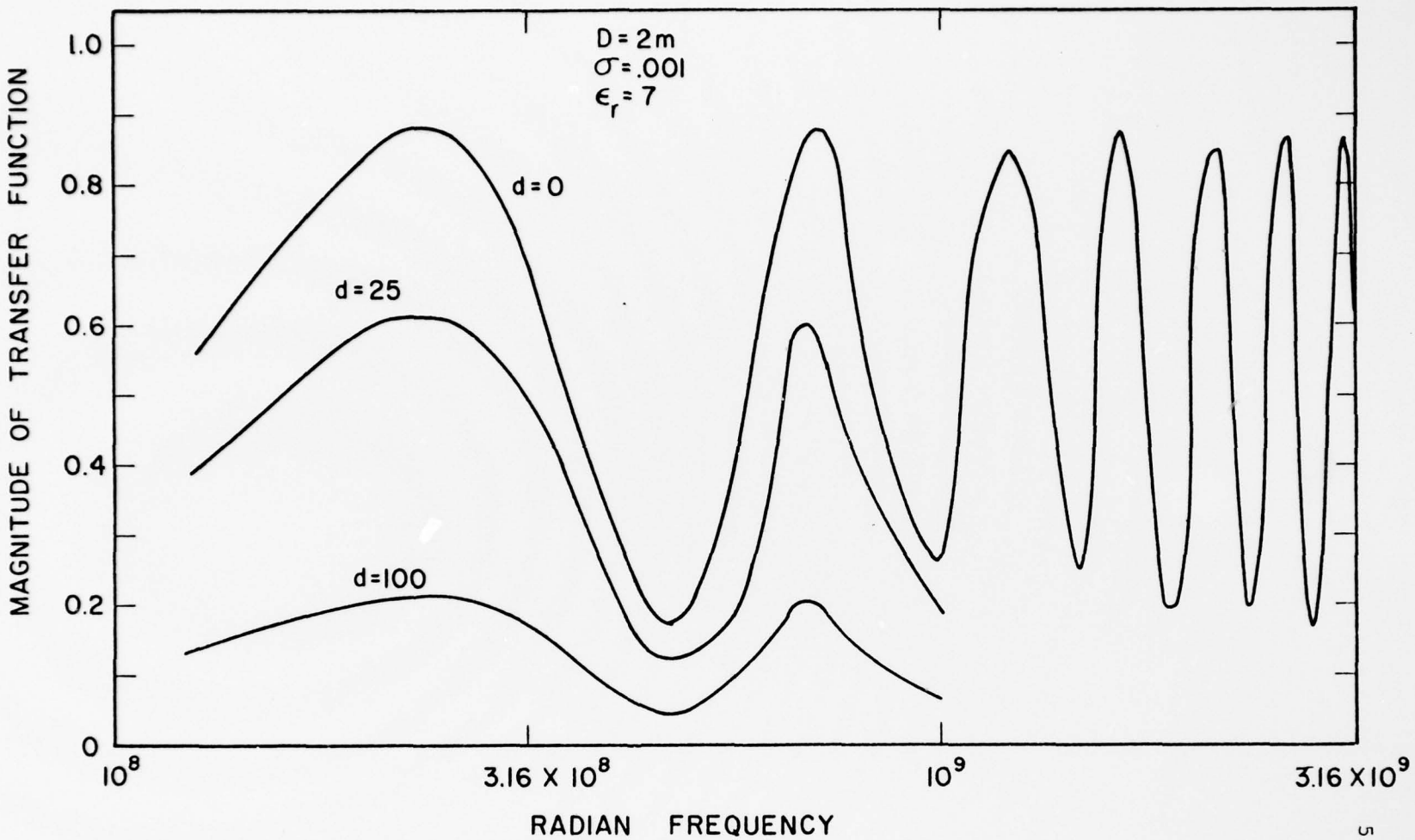

FIGURE 1 TRANSFER FUNCTION FOR REFLECTIONS FROM A BURIED TUNNEL

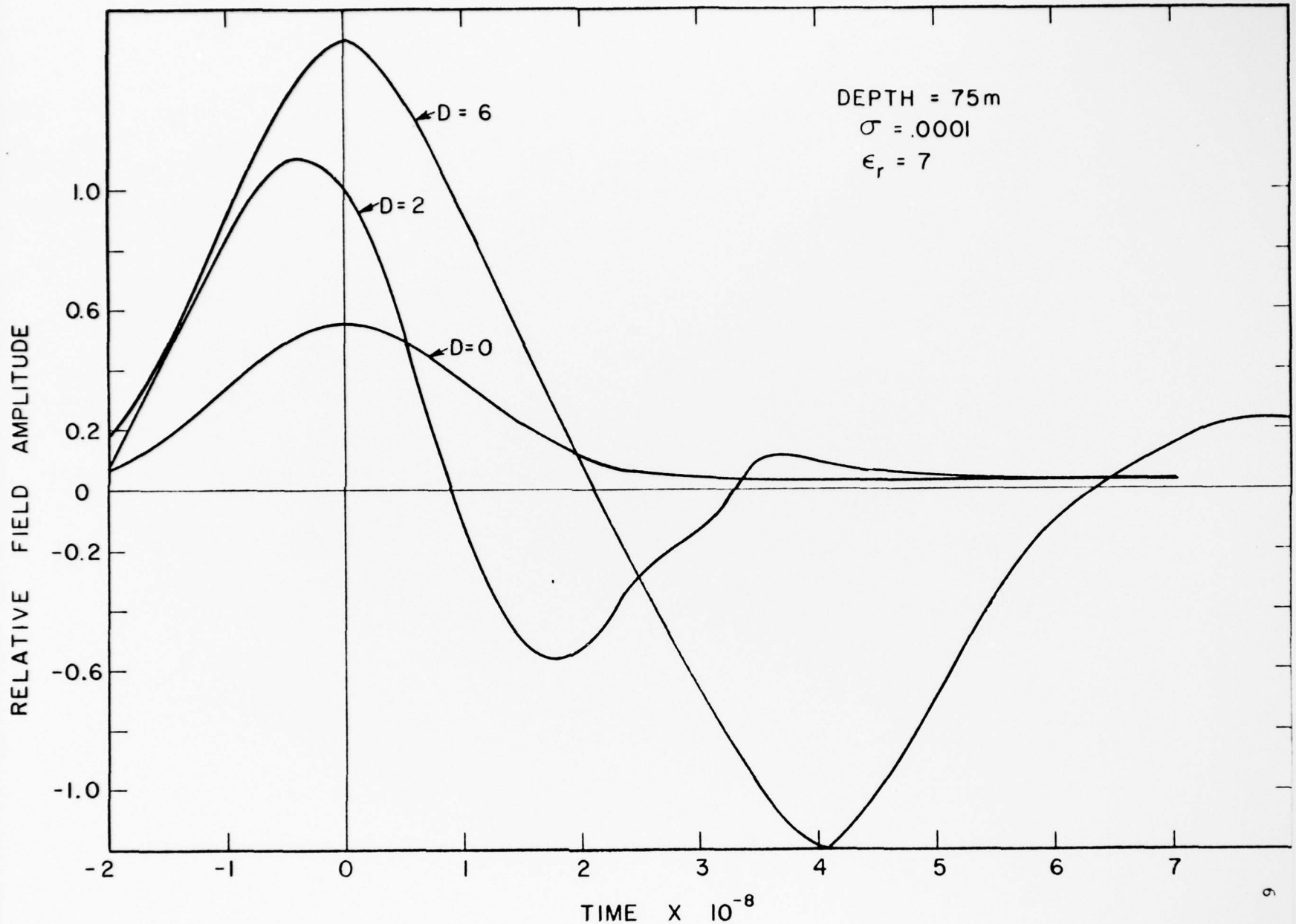

FIGURE 2 TIME DOMAIN REFLECTED PULSE FROM DIFFERENT SIZE TUNNELS (DEPTH = 75M)

the earth near a buried tunnel is shown in Figure 3. This figure can be understood by referring to the actual physical arrangement shown in Figure 4. When the antenna is on the left the physical distance to the tunnel is greater than when the sound is overhead. The high numbers in Figure 3 represent tunnel reflections and present a generally hyperbolic trace. The small sketch on Figure 4 shows this diagrammatically. Using the maximum number that appears on Figure 3 a gray scale from zero to maximum optical density can be constructed. This is also illustrated on the right in Figure 3. Note that the density variations correspond to the maximum and minimum amplitudes on the time response curve shown in Figure 2. More detail than shown on Figure 3 is possible if a gray scale with narrower individual limits is chosen. Although it is very easy to recognize a tunnel from this picture, noise, clutter, blocking layers, and multiple targets make practical identification very difficult. Conventional methods for tunnel detection would use individual signals and frequency sensitive filters.

The basic tunnel detection scheme used in our study involved a new concept in interpreting soundings. A "geometrical filter" was used to detect tunnels from the sounding. Inverse reconstruction might also be a good name for the method. Real space reconstructions[2] have been used recently to reconstruct a three dimensional image from a set of two dimensional projections. As with classic Fourier reconstructions, the more views of an object that are available, the greater the definition of the

MODEL: SINGLE TUNNEL

1.0	0.0	0.0	1.0	2.0	1.0	0.0	0.0	1.0
0.0	1.0	1.0	0.0	6.0	0.0	1.0	1.0	0.0
1.0	0.0	0.0	2.0	16.0	2.0	0.0	0.0	1.0
0.0	0.0	1.0	6.0	40.0	6.0	1.0	0.0	0.0
1.0	0.0	0.0	17.0	74.0	17.0	0.0	0.0	1.0
0.0	0.0	1.0	41.0	97.0	41.0	1.0	0.0	0.0
0.0	1.0	1.0	74.0	88.0	74.0	1.0	1.0	0.0
0.0	0.0	1.0	96.0	45.0	96.0	1.0	0.0	0.0
0.0	1.0	3.0	86.0	10.0	86.0	3.0	1.0	0.0
1.0	0.0	7.0	42.0	46.0	42.0	7.0	0.0	1.0
0.0	1.0	21.0	12.0	47.0	12.0	21.0	1.0	0.0
0.0	0.0	47.0	46.0	24.0	46.0	47.0	0.0	0.0
0.0	1.0	78.0	45.0	1.0	45.0	78.0	1.0	0.0
0.0	0.0	92.0	23.0	9.0	23.0	92.0	0.0	0.0
0.0	0.0	74.0	0.0	8.0	0.0	74.0	0.0	0.0
0.0	1.0	26.0	9.0	5.0	9.0	26.0	1.0	0.0
0.0	1.0	23.0	8.0	4.0	8.0	23.0	1.0	0.0
0.0	2.0	46.0	5.0	4.0	5.0	46.0	2.0	0.0
0.0	6.0	39.0	4.0	3.0	4.0	39.0	6.0	0.0
0.0	16.0	15.0	4.0	2.0	4.0	15.0	16.0	0.0
0.0	38.0	3.0	3.0	3.0	3.0	3.0	38.0	0.0
0.0	67.0	9.0	2.0	4.0	2.0	9.0	67.0	0.0
0.0	85.0	7.0	3.0	3.0	3.0	7.0	85.0	0.0
0.0	74.0	5.0	4.0	3.0	4.0	5.0	74.0	0.0
0.0	34.0	4.0	3.0	2.0	3.0	4.0	34.0	0.0
1.0	14.0	4.0	2.0	3.0	2.0	4.0	14.0	1.0
0.0	41.0	3.0	2.0	4.0	2.0	3.0	41.0	0.0
1.0	39.0	2.0	3.0	3.0	3.0	2.0	39.0	1.0
0.0	18.0	3.0	4.0	2.0	4.0	3.0	18.0	0.0

NUMERICAL OUTPUT

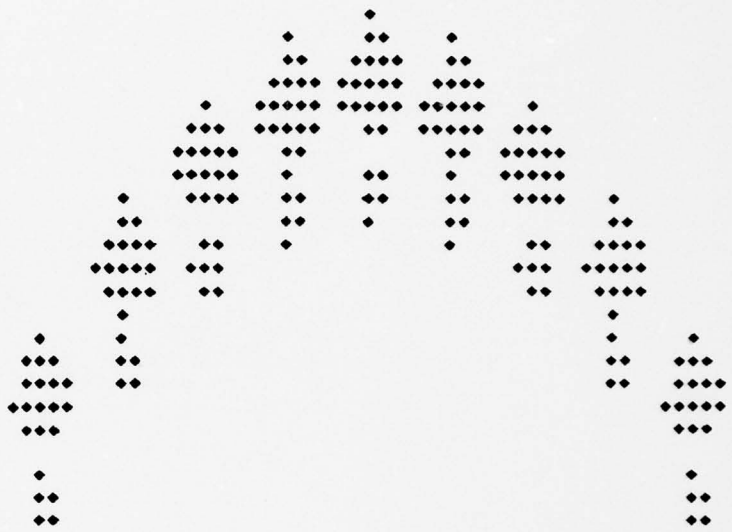

GREY SCALE OUTPUT

FIGURE 3 THEORETICALLY GENERATED VIDEO PULSE SOUNDING FOR A BURIED TUNNEL

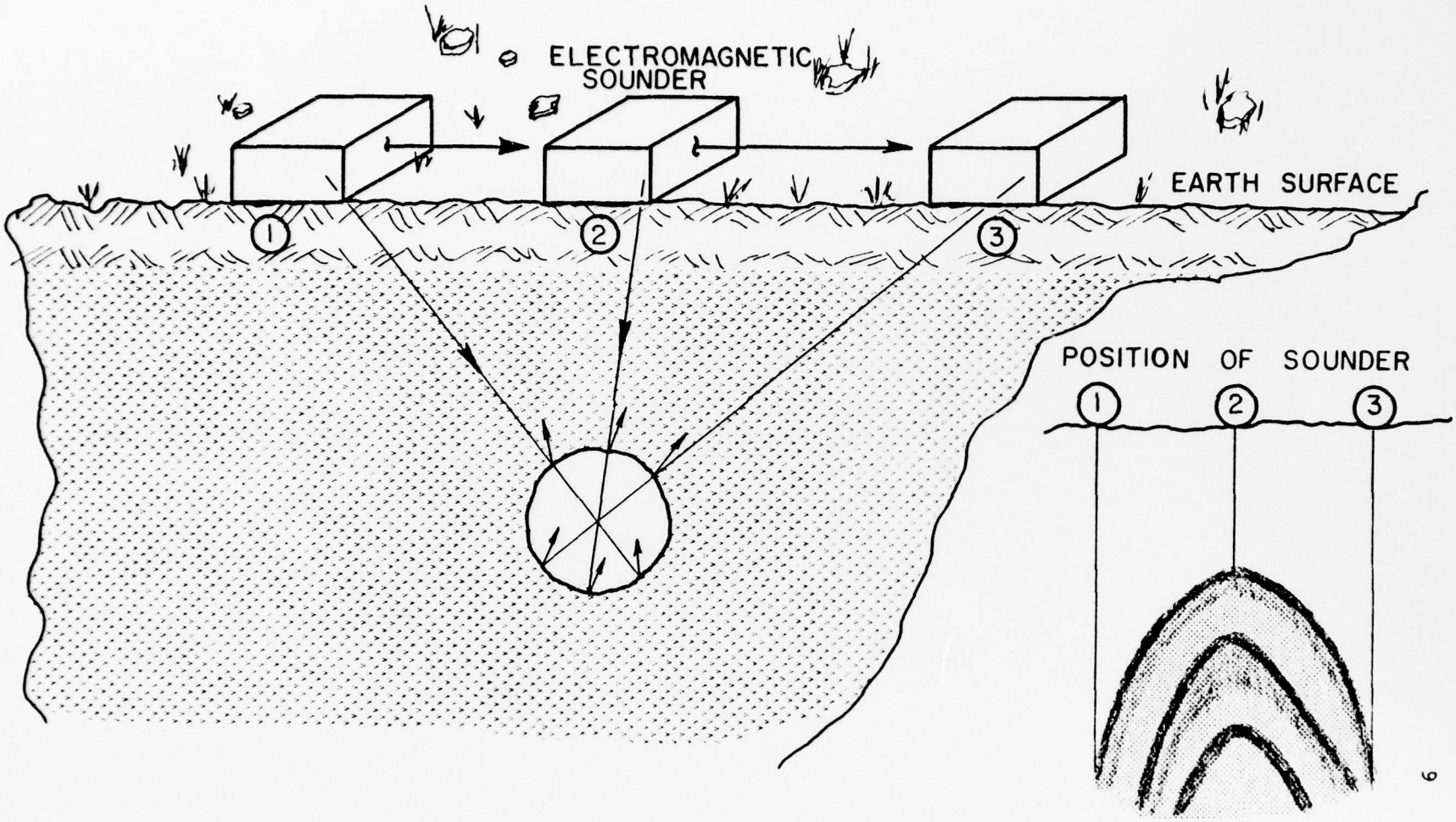

FIGURE 4 PHYSICAL ARRANGEMENT OF THE VIDEO PULSE RADAR SYSTEM

reconstruction. Tunnel identification is achieved as follows:

1. Two pseudo-projections (each one dimensional) are formed at two different viewing angles from the sounding.

2. The pseudo-projections are used to reconstruct the sounding.

The angles for the pseudo-projections are chosen so as to reconstruct the tunnel aspects of the sounding to a high degree of accuracy. Intervening layers and clutter are reconstructed to a low degree of accuracy with the reconstruction method (or algorithm). The result is that a "geometrical" filter has been developed which basically sees only tunnel tracings.

The final reconstructions show the details of minor pulse peaks which are related to the tunnel size and the surrounding material. The tunnel has a unique pattern which is emphasized by the reconstruction. Note that the sounding picture reconstruction is very successful at retaining tunnel attributes in the presence of large amounts of extraneous signals.

Figures 5, 6 and 7 are geometrical filter versions of the single tunnel sounding of Figure 3. The pseudo-projection angles are ±14°, ±20°, ±30°. In all cases the numerical (left) and grey scale (right) outputs show two dominant features; a central core plus two oblique skirts. The grey scale dots are actually maxima or minima since only the absolute value of the

MODEL: SINGLE TUNNEL
PHI = 14°

```
  0.0   0.0   0.3   6.2  11.6   6.2   0.3   0.0   0.0
    0.0   0.2   4.0  36.9  36.9   4.0   0.2   0.0
  0.0   0.1   2.3  23.6 117.3  23.6   2.3   0.1   0.0
    0.1   2.0  13.5  75.1  75.1  13.5   2.0   0.1
  0.1   1.6  11.7  42.9  48.1  42.9  11.7   1.6   0.1
    1.6   9.8  37.2  27.4  27.4  37.2   9.8   1.6
  1.5   9.7  31.0  23.8  15.7  23.8  31.0   9.7   1.5
    9.0  30.6  19.8  13.6  13.6  19.8  30.6   9.0
  5.6  28.7  19.6  11.3  11.8  11.3  19.6  28.7   5.6
    17.8  18.3  11.2   9.8   9.8  11.2  18.3  17.8
 28.3  11.4  10.5   9.7   8.2   9.7  10.5  11.4  28.3
    18.1   6.5   9.1   8.1   8.1   9.1   6.5  18.1
 10.8  10.4   5.6   7.6   8.0   7.6   5.6  10.4  10.8
    6.2   9.0   4.7   7.5   7.5   4.7   9.0   6.2
  1.6   5.4   7.5   4.6   7.0   4.6   7.5   5.4   1.6
    1.4   4.5   7.4   4.3   4.3   7.4   4.5   1.4
  0.1   1.1   4.4   6.9   2.7   6.9   4.4   1.1   0.1
    0.1   1.1   4.1   4.3   4.3   4.1   1.1   0.1
  0.0   0.0   1.0   2.6   6.9   2.6   1.0   0.0   0.0
    0.0   0.0   0.6   4.1   4.1   0.6   0.0   0.0
  0.0   0.0   0.0   1.0   2.4   1.0   0.0   0.0   0.0
```

NUMERICAL OUTPUT

```
THE TUNNEL IS AT  9, 3   SUM IS  68.5
THE TUNNEL IS AT 17,11   SUM IS  21.4
THE TUNNEL IS AT  1,11   SUM IS  21.4
THE TUNNEL IS AT  9,19   SUM IS   4.7
```

GREY SCALE OUTPUT

FIGURE 5 SUBSURFACE SOUNDING AFTER GEOMETRICAL FILTERING (PHI = 14°)

MODEL: SINGLE TUNNEL
PHI = 20°

```
 0.0   0.0   0.4   0.3   0.3   0.3   0.4   0.0   0.0
   0.0   0.3   1.0   1.5   1.5   1.0   0.3   0.0
 0.0   0.3   0.8   5.5   7.3   5.5   0.8   0.3   0.0
   0.1   0.8   4.4  26.7  26.7   4.4   0.8   0.1
 0.1   0.4   4.1  21.3  98.3  21.3   4.1   0.4   0.1
   0.4   2.1  19.7  78.5  78.5  19.7   2.1   0.4
 0.2   2.1  10.2  72.6  62.7  72.6  10.2   2.1   0.2
   0.9  10.3  37.4  58.0  58.0  37.4  10.3   0.9
 1.7   4.5  38.0  29.9  53.6  29.9  38.0   4.5   1.7
   8.4  16.5  30.3  27.7  27.7  30.3  16.5   8.4
 5.1  30.9  13.2  28.0  14.3  28.0  13.2  30.9   5.1
  18.9  24.7  12.2  14.5  14.5  12.2  24.7  18.9
14.9  15.1  22.8   6.3  14.7   6.3  22.8  15.1  14.9
  11.9  14.0  11.8   6.4   6.4  11.8  14.0  11.9
23.0  11.0   7.2  12.0   2.8  12.0   7.2  11.0  23.0
  21.2   5.7   7.3   5.2   5.2   7.3   5.7  21.2
15.7  11.0   5.8   3.2   9.7   3.2   5.8  11.0  15.7
   8.1  11.1   2.5   5.9   5.9   2.5  11.1   8.1
 8.6   8.2   4.8   4.7   3.6   4.7   4.8   8.2   8.6
   8.8   3.6   9.1   2.9   2.9   9.1   3.6   8.8
 1.7   3.8   6.7   5.5   2.3   5.5   6.7   3.8   1.7
   0.7   7.1   4.1   4.4   4.4   4.1   7.1   0.7
 0.5   1.4   4.4   3.2   8.4   3.2   4.4   1.4   0.5
   1.0   0.8   3.4   6.2   6.2   3.4   0.8   1.0
 0.0   0.6   0.7   6.6   4.6   6.6   0.7   0.6   0.0
   0.0   0.5   1.3   4.9   4.9   1.3   0.5   0.0
 0.0   0.0   0.9   1.0   5.2   1.0   0.9   0.0   0.0
   0.0   0.0   0.7   1.0   1.0   0.7   0.0   0.0
 0.0   0.0   0.0   0.7   0.2   0.7   0.0   0.0   0.0
   0.0   0.0   0.0   0.1   0.1   0.0   0.0   0.0
 0.0   0.0   0.0   0.0   0.1   0.0   0.0   0.0   0.0
```

CUMULATIVE OUTPUT

```
THE TUNNEL IS AT  9, 5    SUM IS  61.9
THE TUNNEL IS AT 15,11    SUM IS  19.9
THE TUNNEL IS AT  3,11    SUM IS  19.9
THE TUNNEL IS AT  9,17    SUM IS   6.4
THE TUNNEL IS AT 12,20    SUM IS   6.2
THE TUNNEL IS AT  6,20    SUM IS   6.2
THE TUNNEL IS AT  9,23    SUM IS   5.9
```

GREY SCALE OUTPUT

FIGURE 6 SUBSURFACE SOUNDING AFTER GEOMETRICAL FILTERING (PHI = 20°)

MODEL: SINGLE TUNNEL
PHI = 30°

```
 0.0   0.0   0.0   0.0   0.0   0.0   0.0   0.0   0.0
   0.0   0.1   0.1   0.0   0.0   0.1   0.1   0.0
 0.0   0.2   0.2   0.1   0.1   0.1   0.2   0.2   0.0
   0.1   0.4   0.5   0.4   0.4   0.5   0.4   0.1
 0.1   0.3   0.9   1.5   2.0   1.5   0.9   0.3   0.1
   0.3   0.7   2.8   7.3   7.3   2.8   0.7   0.3
 0.3   0.7   2.2  13.2  26.1  13.2   2.2   0.7   0.3
   0.6   2.0  10.6  47.3  47.3  10.6   2.0   0.6
 0.6   1.7   9.7  38.0  85.7  38.0   9.7   1.7   0.6
   1.8   7.9  34.8  68.7  68.7  34.9   7.9   1.8
 1.1   8.7  28.5  63.1  55.1  63.1  28.5   8.7   1.1
   5.2  31.2  51.5  50.6  50.6  51.5  31.2   5.2
 3.0  18.7  56.5  41.4  46.5  41.4  56.5  18.7   3.0
  10.6  33.8  45.3  38.0  38.0  45.3  33.9  10.6
19.5  19.2  27.1  41.6  31.0  41.6  27.2  19.3  19.6
  35.4  15.4  24.9  34.0  34.0  24.9  15.5  35.4
23.1  28.4  14.2  20.4  37.2  20.4  14.2  28.4  23.2
  18.5  26.1  11.6  22.3  22.3  11.6  26.1  18.6
 9.9  17.0  21.3  12.7  13.4  12.7  21.3  17.1  10.0
   9.1  13.9  23.3   7.6   7.6  23.4  13.9   9.2
14.8   7.5  15.2  14.0   4.3  14.0  15.3   7.5  14.9
  12.1   8.2   9.1   8.0   8.0   9.1   8.2  12.2
19.6  13.3   4.9   5.2  14.6   5.2   4.9  13.3  19.7
  21.5   8.0   2.8   9.6   9.6   2.8   8.0  21.6
22.2  12.9   4.5   5.1   6.2   5.1   4.5  12.9  22.3
  13.3   7.3   8.3   3.4   3.4   8.3   7.4  13.3
 5.6   7.6  13.5   5.4   1.8   5.5  13.5   7.6   5.6
   3.2  13.9   8.8   2.9   2.9   8.8  14.0   3.2
 5.2   5.9   9.1   4.7   4.8   4.7   9.1   5.9   5.2
   9.6   3.8   4.9   7.7   7.7   4.9   3.9   9.6
 6.4   6.2   2.1   7.9  12.5   7.9   2.1   6.3   6.4
   4.2   3.4   3.4  12.9  12.9   3.4   3.4   4.2
 1.3   2.2   5.5   5.4  13.3   5.4   5.5   2.2   1.3
   0.7   3.5   8.8   5.6   5.6   8.8   3.7   0.7
 1.0   1.2   5.9   9.1   2.4   9.1   5.9   1.2   1.0
   1.5   1.9   6.1   3.9   3.9   6.1   1.9   1.6
 0.3   2.5   1.9   2.6   6.3   2.6   1.9   2.5   0.3
   0.5   2.6   0.8   4.2   4.2   0.8   2.6   0.5
 0.0   0.5   1.1   1.3   2.8   1.3   1.1   0.5   0.0
   0.0   0.2   1.8   0.9   0.9   1.8   0.2   0.0
 0.0   0.0   0.4   1.2   0.3   1.2   0.4   0.0   0.0
   0.0   0.0   0.2   0.4   0.4   0.2   0.0   0.0
 0.0   0.0   0.0   0.1   0.5   0.1   0.0   0.0   0.0
   0.0   0.0   0.0   0.1   0.1   0.0   0.0   0.0
 0.0   0.0   0.0   0.0   0.0   0.0   0.0   0.0   0.0
   0.0   0.0   0.0   0.0   0.0   0.0   0.0   0.0
 0.0   0.0   0.0   0.0   0.0   0.0   0.0   0.0   0.0
   0.0   0.0   0.0   0.0   0.0   0.0   0.0   0.0
 0.0   0.0   0.0   0.0   0.0   0.0   0.0   0.0   0.0
```

CUMULATIVE OUTPUT

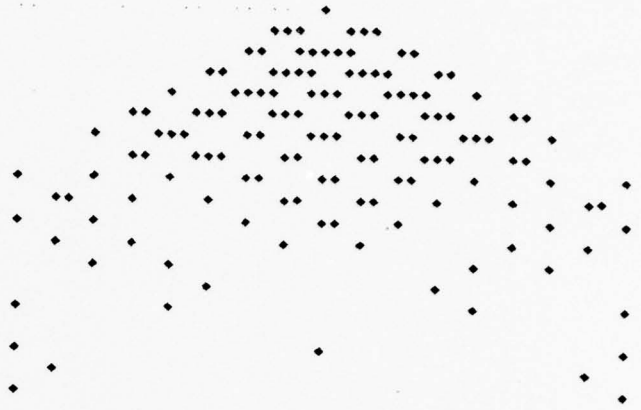

GREY SCALE OUTPUT

FIGURE 7 SUBSURFACE SOUNDING AFTER GEOMETRICAL FILTERING (PHI = 30°)

signal is involved. The most useful output is Figure 6 since the detailed attributes of the skirt are most clearly shown. These skirts contain the basic information about the size and shape of the tunnel. The central core region gives basic target information about the physical location of the tunnel. The computer grey scale sounding for a single tunnel with a layer and lower blotch is shown in Figure 8. A geometrically filtered output for this case is shown in Figure 9. Note that only the tunnel attributes are preserved by the picture detection process.

A noise equal to 25 and 50% of the signal tunnel signal was added to the sounding of Figure 3. The geometrically filtered outputs of Figures 10 and 11 show that even in these extreme cases the pictorial tunnel attributes are evident. Even when the added noise is raised to 100 percent the geometrically filtered output of Figure 12 clearly shows the power of the detection method.

Two separated tunnels were also used to test the detection algorithm. The geometrically filtered outputs are shown in Figures 13, 14 and 15 for the original noiseless sounding and for 50 and 100 percent additive noise. Again the tunnels are clearly evident.

It can be concluded that the pictorial detection schemes is uniquely able to locate and classify buried tunnels under a variety of conditions including high noise and clutter values.

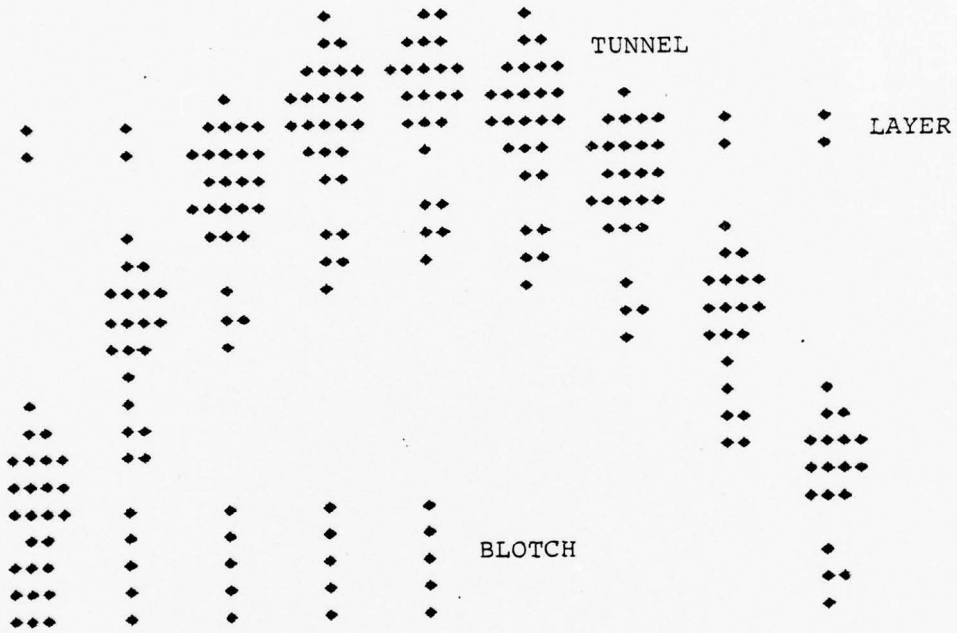

FIGURE 8 VIDEO PULSE SOUNDING FROM A BURIED TUNNEL WITH LAYER AND BLOTCH

MODEL: SINGLE TUNNEL PLUS LAYER AND BLOTCH
PHI = 18°

```
 0.0   0.0   0.5   4.9   1.4   4.7   0.5   0.0   0.0
   0.0   0.5   8.2   6.7   6.5   7.6   0.4   0.0
 0.0   0.2   7.0  11.1  32.0  10.5   6.3   0.3   0.0
   0.2   3.6   9.5  53.4  51.9   8.8   4.0   0.3
 0.2   3.6   5.0  45.7  86.6  43.4   5.6   4.0   0.2
   2.5   4.9  23.8  74.0  72.4  27.4   5.5   2.9
 2.8   3.4  23.7  38.6  61.9  45.7  27.2   4.0   3.1
   3.9  16.1  38.4  32.2  39.1  45.3  19.8   4.3
 4.5  18.5  26.1  32.1  20.4  38.7  33.0  21.2   3.7
  21.5  30.0  21.8  20.3  20.2  28.2  35.3  18.1
13.8  34.8  25.1  13.8  20.1  14.7  30.2  30.1   7.1
  22.3  29.1  15.8  13.7  14.6  15.7  25.8  11.9
30.8  18.6  18.4  15.7   9.9  15.7  13.4  10.2  18.5
  25.7  11.8  18.2  11.4  10.6  13.4   5.3  15.8
30.9  16.3  11.7  13.2  12.2   9.1   5.3   8.3  15.9
  19.5  16.1   8.5  14.2  10.4   3.6   8.2   8.3
15.6  19.3  11.7   9.1  12.1   4.1   5.6   8.2   6.8
  15.5  14.1  12.5   7.8   4.8   6.4   5.6   6.8
 2.3  11.3  15.1  10.7   3.1   7.5   6.4   4.6   1.5
   1.7  12.1  12.9   4.2   4.8   7.5   5.3   1.0
 0.8   1.8  10.3   5.1   6.6   4.8   6.2   1.1   0.5
   0.8   1.5   4.1   7.9   6.6   4.0   1.3   0.6
 0.0   0.7   0.6   6.3   7.9   5.5   0.8   0.6   0.0
   0.0   0.3   0.9   6.3   6.6   1.2   0.4   0.0
 0.0   0.0   0.4   0.9   5.3   1.4   0.6   0.0   0.0
   0.0   0.0   0.4   0.8   1.1   0.7   0.0   0.0
 0.0   0.0   0.0   0.4   0.2   0.6   0.0   0.0   0.0
```

NUMERICAL OUTPUT

```
THE TUNNEL IS AT  9, 5   SUM IS  67.9
THE TUNNEL IS AT 17,13   SUM IS  15.4
THE TUNNEL IS AT  3,11   SUM IS  27.5
THE TUNNEL IS AT 11,19   SUM IS   6.2
THE TUNNEL IS AT  1,13   SUM IS  26.3
THE TUNNEL IS AT  9,21   SUM IS   6.0
```

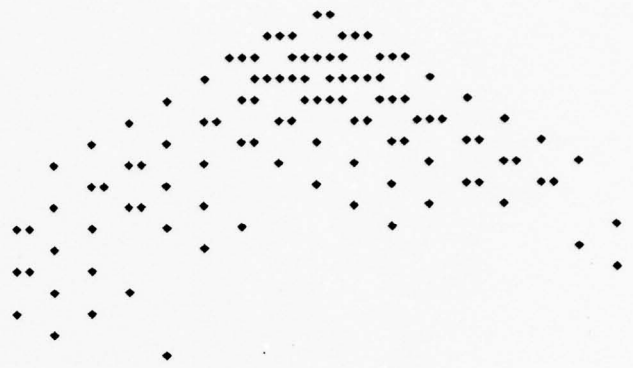

GREY SCALE OUTPUT

FIGURE 9 RECONSTRUCTED IMAGE OF BURIED TUNNEL WITH LAYER AND BLOTCH

MODEL: SINGLE TUNNEL PLUS RANDOM NOISE = 25% OF MAXIMUM SIGNAL
PHI = 18°

```
16.0  21.3  24.2  27.6   6.8  21.5  25.0  30.2   9.0
   13.7  21.4  40.6  18.0  19.0  26.7  24.3  23.5
13.6  13.8  35.9  26.4  50.0  23.6  26.0  18.9  20.3
   13.7  23.1  23.4  73.4  62.1  23.0  20.2  16.4
 8.8  22.9  15.0  65.0  91.1  60.5  17.9  17.5  12.8
   14.8  14.9  41.8  80.7  88.7  47.0  15.4  13.7
18.5   9.6  41.5  51.9  78.6  69.0  40.7  12.1  12.0
   12.0  26.7  51.5  50.6  61.2  59.7  31.9  10.6
11.6  33.5  33.2  50.1  39.3  52.9  46.8  27.9  12.9
   31.3  41.6  32.3  39.0  34.0  41.5  41.0  33.9
31.9  38.8  40.5  25.1  33.7  26.7  36.3  49.7  25.5
   39.6  37.8  31.5  21.7  26.5  23.4  44.1  37.4
48.3  38.5  29.4  27.2  17.1  23.2  28.3  33.1  45.1
   47.0  30.0  25.4  21.4  14.9  28.1  21.3  40.0
36.0  36.6  25.9  20.0  18.7  18.1  21.1  25.7  34.0
   28.0  31.6  20.3  17.5  22.7  13.6  25.5  21.9
31.2  24.2  24.8  17.3  21.2  17.1  16.4  21.7  26.9
   27.0  19.0  21.7  21.6  15.9  20.6  14.0  26.7
22.8  21.2  16.6  26.4  16.2  19.2  17.5  17.2  22.9
   17.9  18.5  20.2  19.8  19.6  16.3  21.6  14.8
21.2  15.6  22.5  15.1  23.9  16.7  20.1  18.5  17.0
   18.5  19.0  16.9  18.3  20.3  20.5  17.3  21.3
15.1  22.5  14.3  20.4  15.5  25.0  17.6  19.9  23.4
   18.3  16.9  17.2  17.3  19.1  21.5  20.3  21.9
20.7  13.8  20.4  14.6  21.4  16.5  24.8  22.3  23.3
   15.6  16.6  17.3  18.0  18.4  18.9  27.2  23.8
15.9  18.8  14.1  21.3  15.5  21.1  20.8  29.0  39.8
```

NUMERICAL OUTPUT


```
THE TUNNEL IS AT 10, 6    SUM IS  77.8
THE TUNNEL IS AT 15,11    SUM IS  41.2
THE TUNNEL IS AT  5,11    SUM IS  36.7
THE TUNNEL IS AT 10,16    SUM IS  19.6
THE TUNNEL IS AT  3,13    SUM IS  38.6
THE TUNNEL IS AT  8,18    SUM IS  20.6
```

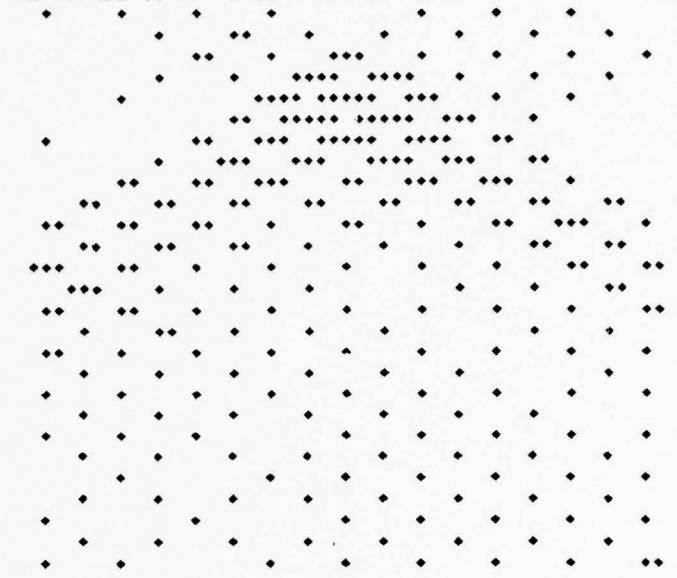

GREY SCALE OUTPUT

FIGURE 10 GEOMETRICALLY FILTERED OUTPUT OF BURIED TUNNEL PLUS RANDOM NOISE (25% OF MAX SIGNAL)

MODEL: SINGLE TUNNEL PLUS RANDOM NOISE = 50% OF MAXIMUM SIGNAL
PHI = 18°

```
30.0  38.6  43.8  53.3  18.8  41.8  42.3  54.9  17.0
   27.4  39.8  73.3  35.5  35.1  45.4  44.6  49.3
28.0  28.2  66.6  48.8  66.3  38.1  47.9  40.0  41.4
   28.9  47.2  44.3  91.2  72.0  40.2  42.9  33.6
19.0  48.3  31.4  82.8  99.1  75.9  36.1  36.1  28.3
   31.8  32.2  58.7  90.0 104.5  68.1  30.3  30.4
41.0  21.1  60.1  63.8  94.9  93.7  57.2  25.6  26.1
   27.3  39.5  65.3  67.2  85.1  78.8  48.2  41.9
24.5  51.0  42.9  68.9  60.3  71.5  66.4  41.4  26.6
   45.8  55.4  45.3  61.7  50.7  60.3  57.0  50.3
52.4  49.7  58.4  40.6  51.9  42.7  51.8  69.2  40.5
   56.9  52.5  52.4  34.1  43.7  36.7  62.9  55.7
66.2  60.0  47.0  44.0  28.8  37.6  44.5  50.6  63.4
   69.8  53.8  39.5  37.1  24.7  45.6  35.8  57.6
50.9  62.6  45.2  33.3  31.9  30.0  36.7  40.8  47.1
   45.6  52.6  38.1  28.6  38.7  24.1  41.8  33.4
52.6  38.4  44.3  32.8  34.8  31.1  27.5  34.2  43.2
   43.9  32.3  38.1  39.8  28.0  35.4  22.5  44.2
40.5  37.0  27.8  46.2  32.0  31.8  29.0  29.1  41.4
   34.1  31.8  33.7  37.2  36.4  26.1  37.5  27.2
41.0  29.3  38.6  27.1  42.3  29.8  33.7  35.1  31.8
   35.2  35.6  31.0  30.9  34.7  38.6  31.6  41.0
29.1  42.7  28.6  35.3  25.3  44.8  36.1  36.8  45.0
   35.4  34.4  32.6  28.9  32.7  42.0  42.1  40.4
39.7  28.4  39.1  26.7  37.4  30.6  49.0  46.3  42.5
   32.0  32.4  32.0  34.5  35.0  35.7  53.8  48.6
30.8  36.4  26.5  41.4  32.3  40.9  39.2  56.5  76.7
```

NUMERICAL OUTPUT


```
THE TUNNEL IS AT  9, 7   SUM IS  88.5
THE TUNNEL IS AT 14,12   SUM IS  55.8
THE TUNNEL IS AT  5,11   SUM IS  52.8
THE TUNNEL IS AT 10,16   SUM IS  33.3
THE TUNNEL IS AT  3,13   SUM IS  58.6
THE TUNNEL IS AT  8,18   SUM IS  37.1
```

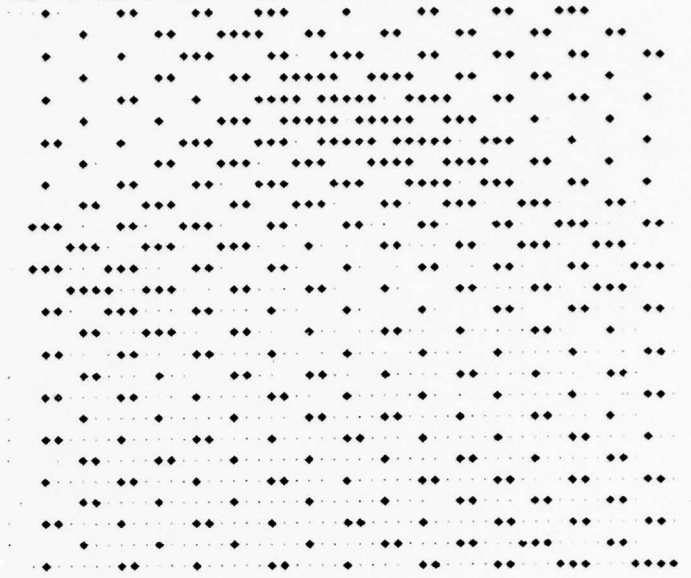

GREY SCALE OUTPUT

FIGURE 11 GEOMETRICALLY FILTERED OUTPUT OF BURIED TUNNEL PLUS RANDOM NOISE (50% OF MAX SIGNAL)

MODEL: SINGLE TUNNEL PLUS RANDOM NOISE = 100% OF MAXIMUM SIGNAL
PHI = 18°

```
 61.0  72.6  82.3 106.0  47.0  83.2  75.1 102.6  34.0
    55.7  76.6 135.7  71.0  67.6  80.6  84.5 103.0
 58.6  58.7 126.4  90.8 102.0  65.5  90.8  84.8  85.4
    61.8  96.8  84.6 130.5  98.8  73.7  91.1  70.3
 41.1 102.0  64.8 121.5 126.4 111.2  74.0  75.6  61.7
    67.8  68.2  93.1 117.7 142.3 111.6  61.4  66.3
 90.1  45.3  98.0  90.2 132.5 142.8  92.6  53.9  56.8
    60.3  65.1  95.0 101.5 133.0 118.5  81.3  46.1
 52.8  86.6  63.1 106.9 101.9 110.3 104.0  69.5  55.9
    75.8  83.9  71.0 107.3  84.5  96.9  89.0  84.2
 93.2  73.5  94.4  71.3  89.0  74.2  82.9 107.8  71.2
    90.3  82.7  94.8  59.2  78.1  63.5 100.4  91.1
102.4 101.6  83.0  78.6  51.9  66.8  76.9  84.9 100.5
   115.2 102.0  68.8  69.0  44.4  81.0  65.0  93.6
 81.2 115.6  84.6  60.4  59.0  53.8  68.5  71.7  74.6
    81.5  95.9  74.3  51.7  71.5  45.5  75.5  57.2
 94.4  67.6  84.2  63.5  62.6  60.5  50.2  60.2  75.7
    78.3  59.3  72.0  77.0  53.0  66.7  40.0  79.7
 76.2  68.7  50.8  87.3  65.1  58.4  53.2  53.0  78.1
    66.9  58.8  61.5  73.6  71.8  46.6  70.4  51.9
 81.0  57.2  71.2  52.0  81.4  57.2  61.7  69.0  61.3
    69.3  64.3  60.2  57.4  64.9  75.8  60.4  81.5
 57.7  83.9  58.6  66.4  45.7  85.9  74.2  71.4  89.5
    69.9  70.9  64.7  52.9  60.5  84.1  87.7  78.3
 77.5  59.1  78.3  51.5  70.1  59.3  99.4  96.3  81.7
    65.6  65.2  62.4  68.2  68.7  70.1 109.1 100.4
 60.5  72.3  51.9  82.6  66.8  81.2  76.9 113.8 153.3
```

NUMERICAL OUTPUT


```
THE TUNNEL IS AT 10, 8   SUM IS 124.3
THE TUNNEL IS AT 14,12   SUM IS  90.6
THE TUNNEL IS AT  6,12   SUM IS  84.4
THE TUNNEL IS AT 10,16   SUM IS  61.5
THE TUNNEL IS AT  4,14   SUM IS  97.4
THE TUNNEL IS AT  8,18   SUM IS  71.1
```

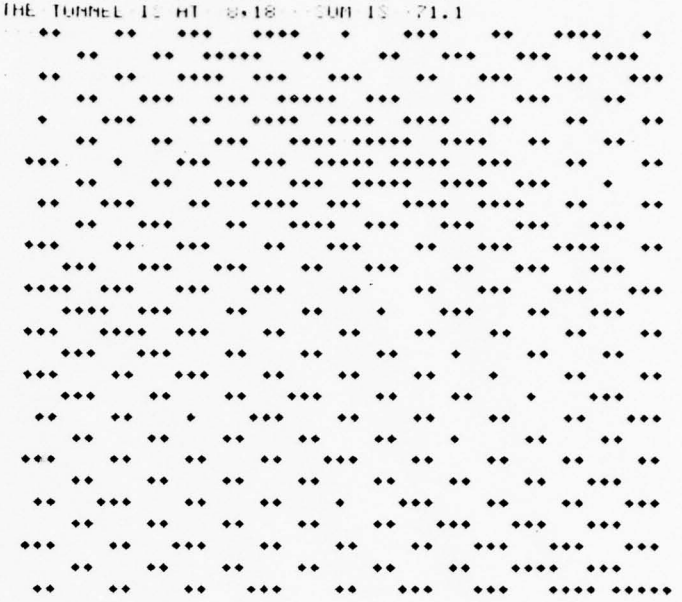

GREY SCALE OUTPUT

FIGURE 12 GEOMETRICALLY FILTERED OUTPUT OF BURIED TUNNEL PLUS RANDOM NOISE (100% OF MAX SIGNAL)

MAGNITUDE OF TRANSFER FUNCTION

MODEL: TWO TUNNELS
PHI = 25°

```
THE TUNNEL IS AT  9.7   SUM IS  70.3
THE TUNNEL IS AT 15.13  SUM IS  22.6
THE TUNNEL IS AT  2.14  SUM IS  32.7
THE TUNNEL IS AT  8.20  SUM IS  10.5
THE TUNNEL IS AT 13.25  SUM IS  49.8
THE TUNNEL IS AT  6.22  SUM IS   9.1
THE TUNNEL IS AT 11.27  SUM IS  43.1
THE TUNNEL IS AT  2.26  SUM IS   5.1
THE TUNNEL IS AT  7.31  SUM IS  23.8
THE TUNNEL IS AT  3.35  SUM IS  19.8
```

```
 0.0   0.0   0.2   0.1   0.2   0.1   0.2   0.0   0.0
   0.0   0.3   0.7   0.6   0.6   0.6   0.3   0.0
 0.0   0.2   0.9   3.1   2.3   2.9   0.8   0.2   0.0
   0.2   0.7   4.0  11.3  10.7   3.6   0.6   0.2
 0.1   0.6   3.0  14.6  52.5  13.5   2.7   0.6   0.1
   0.4   2.7  11.1  68.3  66.2  10.1   2.6   0.4
 0.2   1.6   9.7  51.7  86.1  49.6   9.7   1.8   0.3
   1.1   5.8  45.1  65.2  64.5  47.5   6.8   1.5
 0.6   4.0  27.1  56.9  48.8  61.7  33.4   5.4   0.8
   2.3  18.7  34.2  42.7  46.7  43.5  26.4   2.9
 5.3  10.6  23.5  25.6  40.8  32.9  34.3  14.4   4.6
  24.9  13.3  17.6  24.5  28.7  26.0  18.7  22.4
33.2  31.4  10.0  16.9  17.3  22.7  14.2  29.1  16.0
  41.9  23.6   9.5  11.9  13.6  12.4  22.0  20.8
25.7  31.4  22.5   6.7   9.4   7.4  19.2  15.8  12.2
  19.3  30.0  15.9   5.3   5.1  11.6  13.8   9.3
26.0  18.4  21.1  12.5   2.9   8.0   8.3   8.1  22.5
  24.9  13.0  16.7   6.8   4.5   5.7   4.9  19.6
19.8  17.5  10.2   9.1  10.6   3.2   3.3  11.8  51.0
  14.0  13.8   5.6  14.1   7.6   1.9   8.1  30.7
12.5  11.0   7.5   8.7  10.1   4.5   4.6  21.1  52.0
   9.9   6.0  11.7   6.2   5.9  10.9  11.9  35.7
 5.6   5.4   9.4   8.4   3.7  14.5  28.2  20.2  34.2
   3.0   8.4   6.7   4.9   8.9  37.5  47.8  19.4
 4.0   4.7   6.0   3.9  12.0  23.0  63.6  45.8  19.2
   6.2   3.4   3.5   9.6  31.1  39.1  60.9  45.3
 6.0   4.4   2.0   8.5  24.8  52.7  37.4  60.3  36.8
   4.3   2.6   4.8  22.2  42.1  50.5  37.0  49.0
 1.8   2.5   6.3  12.6  37.6  40.3  50.0  30.1  31.0
   1.1   6.2  16.3  21.3  36.0  39.8  40.6  19.0
 1.5   2.6  16.0  27.7  20.4  35.6  32.4  25.7   5.9
   3.7   6.7  27.1  26.5  20.2  29.0  20.5   8.0
 5.3   9.7  11.3  26.0  26.2  16.4  18.3   6.4  15.2
  13.6  16.5  10.9  25.7  21.3  10.4   5.7  12.1
13.9  23.1  15.8  10.7  20.9  13.5   3.2  10.8   3.0
  23.6  22.2  15.6   8.7  13.2   4.2   6.1   2.7
 5.1  22.6  21.9  12.7   5.5   4.1   8.0   1.5   4.5
   4.9  22.3  17.8   8.0   1.7   7.8   2.0   2.5
 0.0   4.8  18.2  11.3   2.5   3.3   1.9   3.3   2.7
```

NUMERICAL OUTPUT

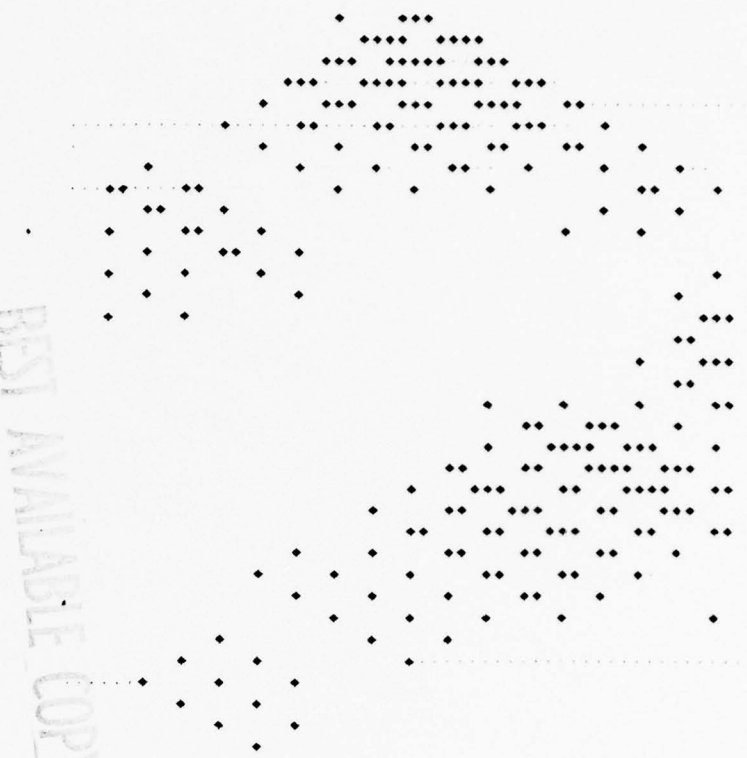

GREY SCALE OUTPUT

FIGURE 13 VIDEO PULSE SOUNDING FROM TWO BURIED TUNNELS

MODEL: TWO TUNNELS PLUS RANDOM NOISE = 50% OF MAXIMUM SIGNAL
PHI = 25°

```
30.0  20.8  29.6  18.3  30.5  26.2  39.1  64.7  17.0
   16.3  39.7  45.5  23.7  24.2  37.7  49.6  59.1
16.2  31.2  61.1  58.8  18.8  34.9  47.9  45.3  52.0
   31.0  47.9  79.1  46.7  27.1  44.3  43.7  39.9
23.0  47.8  62.0  62.8  67.3  34.4  40.5  38.5  38.0
   35.4  61.8  49.2  90.5  85.4  31.5  35.6  36.7
35.1  45.7  49.1  70.9 114.8  78.1  27.7  33.9  32.8
   45.4  36.3  70.7  90.0 105.0  68.7  26.4  30.3
34.0  36.0  52.3  89.7  82.3  92.4  65.5  23.6  26.7
   27.0  51.9  66.4  82.0  72.4  88.0  58.5  20.8
34.4  38.9  65.9  60.7  72.2  69.0  78.7  51.5  23.0
   49.5  49.4  60.2  53.4  68.8  61.7  69.2  57.0
54.7  62.9  45.1  53.0  50.9  61.4  54.3  76.7  50.8
   69.5  57.4  39.7  50.5  45.5  54.1  60.1  68.3
69.5  63.5  50.6  37.9  45.1  40.1  59.9  53.5  52.5
   63.5  55.9  48.2  33.8  39.7  44.4  53.3  41.1
72.3  55.9  53.2  43.1  29.8  44.0  39.5  41.0  44.2
   63.6  53.3  47.6  37.9  33.0  39.2  30.3  44.0
62.7  60.6  47.6  41.9  42.0  29.4  30.1  32.6  84.3
   50.2  54.2  41.9  46.4  37.4  22.6  32.4  62.5
52.6  44.9  47.7  46.4  41.3  28.7  24.2  62.0  67.2
   47.0  39.5  52.8  41.3  31.7  30.9  46.4  66.7
39.3  41.4  43.8  47.0  31.8  34.1  59.1  50.0  64.3
   34.6  45.8  39.0  36.1  34.1  65.3  63.6  48.2
35.0  38.3  40.8  29.9  38.8  65.3  70.3  61.3  51.7
   38.8  34.1  31.4  32.2  74.4  70.3  67.7  65.8
36.8  34.5  26.2  33.7  61.6  80.0  67.8  72.8  52.2
   32.7  26.5  28.1  64.5  66.3  77.1  72.8  57.7
25.7  25.1  28.5  53.9  69.4  63.9  82.9  57.8  56.5
   19.8  27.0  54.6  58.0  67.0  68.6  65.7  56.5
26.2  21.2  51.8  58.7  55.9  71.9  54.4  64.3  48.3
   28.1  40.7  55.7  56.6  60.0  57.0  53.3  55.0
29.6  53.9  43.8  53.7  60.8  47.6  55.8  45.5  65.7
   56.7  58.0  42.2  57.7  48.2  46.6  47.7  54.4
38.8  61.0  55.9  45.3  45.7  47.2  39.8  57.0  41.4
   41.8  58.8  60.0  36.0  44.8  40.4  47.6  43.3
37.7  40.3  63.1  47.6  35.2  38.3  48.2  36.2  75.9
   36.4  43.3  50.1  46.6  30.1  45.7  36.7  63.3
45.9  39.1  34.3  49.0  39.8  36.0  34.8  64.2  27.7
```

NUMERICAL OUTPUT

```
THE TUNNEL IS AT 10, 8    SUM IS  94.7
THE TUNNEL IS AT 15,13    SUM IS  66.3
THE TUNNEL IS AT  1,17    SUM IS  66.5
THE TUNNEL IS AT  6,22    SUM IS  47.5
THE TUNNEL IS AT 11,27    SUM IS  78.6
```

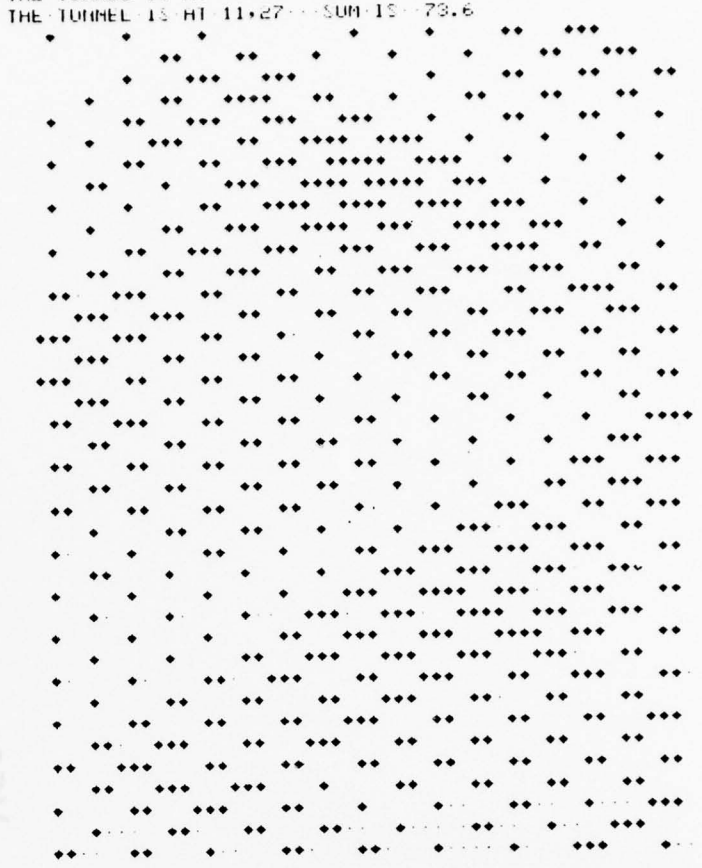

GREY SCALE OUTPUT

FIGURE 14 GEOMETRICALLY FILTERED OUTPUT OF TWO BURIED TUNNELS PLUS RANDOM NOISE (50% OF MAX SIGNAL)

MODEL: TWO TUNNELS PLUS RANDOM NOISE = 100% OF MAXIMUM SIGNAL
PHI = 25°

61.0 40.3 56.8 41.9 75.9 61.9 74.4 125.2 33.9
31.8 77.9 84.7 53.2 56.0 69.1 95.5 120.8
82.8 61.4 116.0 107.6 39.2 62.6 88.7 92.1 105.5
63.4 91.5 147.4 79.4 43.8 80.3 85.6 80.4
48.6 94.5 116.3 108.8 88.7 56.2 77.4 74.7 81.6
72.4 120.1 85.8 121.5 113.8 54.3 67.6 75.8
78.8 91.9 88.6 95.9 155.9 109.8 47.4 68.6 71.3
100.1 67.9 99.0 123.0 150.4 95.9 48.1 64.6
78.2 73.9 75.8 127.0 118.6 131.3 97.3 45.2 59.6
57.8 82.5 97.2 122.5 103.6 133.3 91.6 41.8
64.2 64.5 105.9 93.8 107.0 105.1 125.4 84.6 43.9
71.7 82.8 102.1 81.9 108.6 98.9 115.8 88.9
74.0 92.0 74.8 89.2 83.1 102.2 91.4 121.7 80.9
94.9 88.8 69.7 90.5 78.2 94.4 96.0 110.7
109.9 91.6 77.5 70.7 85.2 72.2 99.1 87.4 86.5
106.0 80.0 78.6 66.6 78.7 75.9 90.2 68.2
116.8 96.6 81.1 74.0 61.5 82.6 69.1 70.4 70.3
102.0 94.0 76.3 68.3 64.6 75.2 53.9 72.6
85.4 103.5 88.4 70.5 71.8 58.8 58.7 55.6 124.9
86.7 97.4 81.7 74.1 65.4 45.9 60.5 95.6
93.7 81.5 89.9 85.8 67.4 51.0 47.3 104.1 90.3
88.2 75.3 94.5 78.1 52.6 52.6 81.4 98.3
77.8 81.5 79.1 86.0 61.0 54.3 90.5 76.9 95.8
71.9 85.6 72.0 67.1 62.9 93.3 85.5 74.9
64.9 75.5 77.9 56.2 69.2 108.1 88.2 83.3 80.6
73.4 68.7 60.8 58.0 119.0 102.1 85.9 89.7
69.8 66.8 53.7 62.7 99.7 112.4 99.5 92.5 71.5
63.5 52.2 55.3 107.8 94.2 109.6 107.1 73.8
56.4 49.6 53.8 95.2 101.8 91.8 118.0 85.5 81.3
44.0 51.1 92.5 89.9 99.2 98.8 94.1 94.1
57.4 45.4 87.9 87.4 87.6 106.8 78.8 103.6 88.4
54.1 78.1 83.0 85.1 94.3 85.2 86.8 97.3
59.3 101.7 73.7 80.9 91.6 75.2 93.9 81.5 113.7
101.9 96.1 71.9 87.1 73.1 82.8 88.2 95.2
66.4 96.3 93.6 77.4 69.5 80.5 77.8 103.0 76.9
62.8 93.8 100.8 61.7 76.5 75.6 90.9 83.2
79.0 61.2 101.0 80.4 68.0 71.9 88.3 73.4 145.0
77.0 65.8 80.6 88.5 63.8 84.0 71.4 127.9
90.6 82.9 52.5 88.7 83.2 74.6 67.8 124.4 51.8

NUMERICAL OUTPUT

THE TUNNEL IS AT 10, 8 SUM IS 138.4
THE TUNNEL IS AT 15,13 SUM IS 106.6
THE TUNNEL IS AT 8,10 SUM IS 113.8
THE TUNNEL IS AT 13,15 SUM IS 91.1
THE TUNNEL IS AT 17,19 SUM IS 97.7
THE TUNNEL IS AT 6,12 SUM IS 94.2
THE TUNNEL IS AT 11,17 SUM IS 75.4
THE TUNNEL IS AT 15,21 SUM IS 88.0
THE TUNNEL IS AT 1,17 SUM IS 108.3
THE TUNNEL IS AT 6,22 SUM IS 87.1
THE TUNNEL IS AT 10,26 SUM IS 101.7
THE TUNNEL IS AT 4,24 SUM IS 79.9
THE TUNNEL IS AT 8,28 SUM IS 93.4

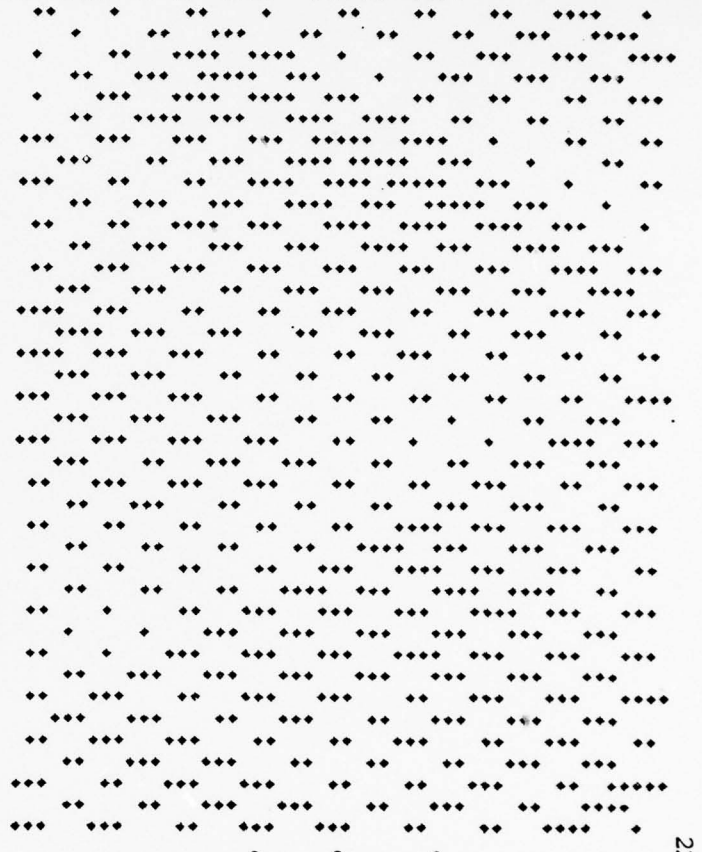

GREY SCALE OUTPUT

FIGURE 15 GEOMETRICALLY FILTERED OUTPUT OF TWO BURIED TUNNELS PLUS RANDOM NOISE (100% MAX SIGNAL)

II. Additional Technical Results

The time domain signal reflected from the tunnel was computed from the steady state transfer function and the frequency spectrum of the pulse. The transfer functions given in Figures 1 to 8 give the plane wave reflected signal for tunnels having diameters from 1 to 5 meters. The conductivities range from 1.2×10^{-3} to 10^{-4} S/m and the relative dielectric constant from $\varepsilon_r = 7$ to $\varepsilon_r = 30$. The tunnel is assumed to be filled with free space. In most cases the rapidly oscillating high frequency range has been truncated.

The geometrical theory of diffraction used in the present theory involves the superposition of the reflections from the top granite tunnel interface and the reflections from the tunnel bottom. Some background results are shown in Figures 9-11. In Figure 9 and 10 the pulse begins in air and is traced through the granite overburden. Figure 11 assumes that the pulse begins in granite and is followed into the granite at different depths. Figures 12 and 13 show the initial tunnel reflection from the upper tunnel interface. Figures 14 and 15 give the pulses from the lower tunnel interface. Since some tunnel signal processing may surpress the top tunnel signal Figure 16 gives the tunnel return signal with and without the first reflection. Figures 17-19 give the full tunnel returned signals for 2 and 7.5 meter tunnels at different depths.

A. Transfer Functions

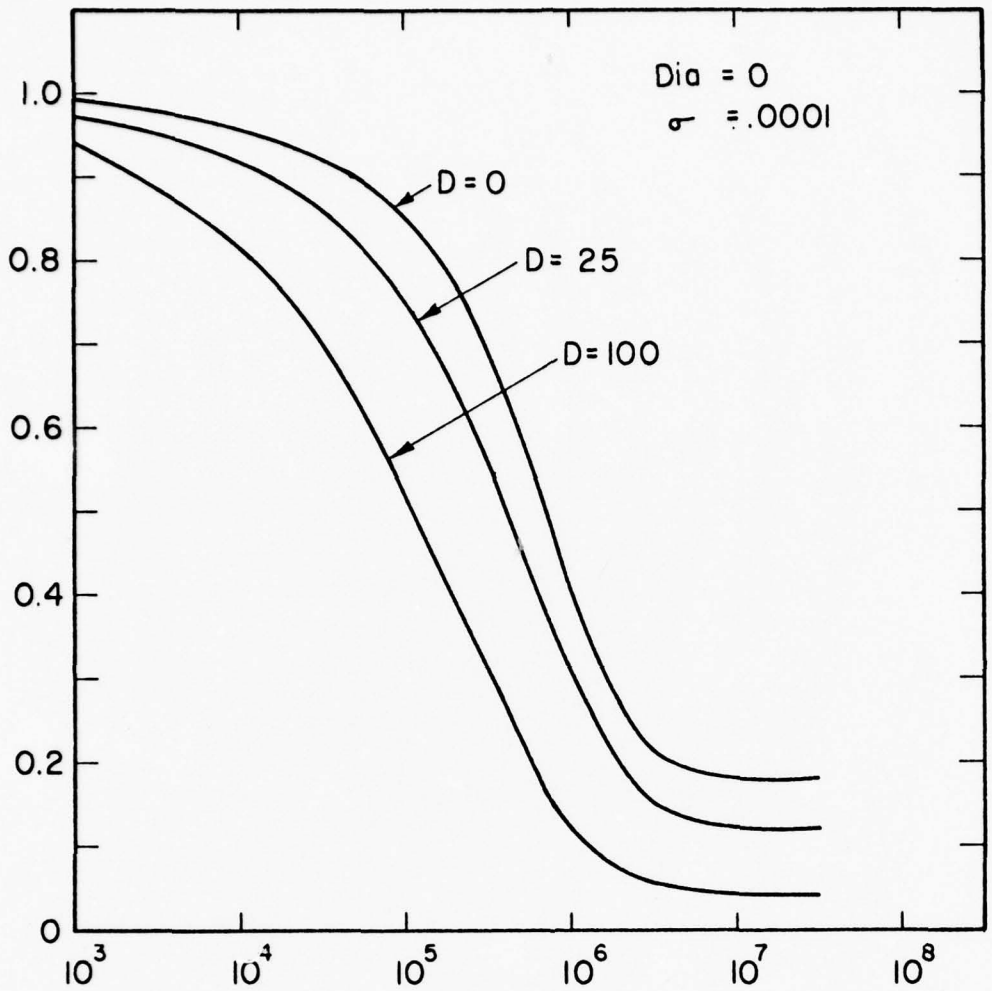

Figure 1 Steady State Transfer Function, diam = 1, $\sigma = 10^{-4}$ S/m, $\varepsilon_r = 7$, D = 0,25,100 m.

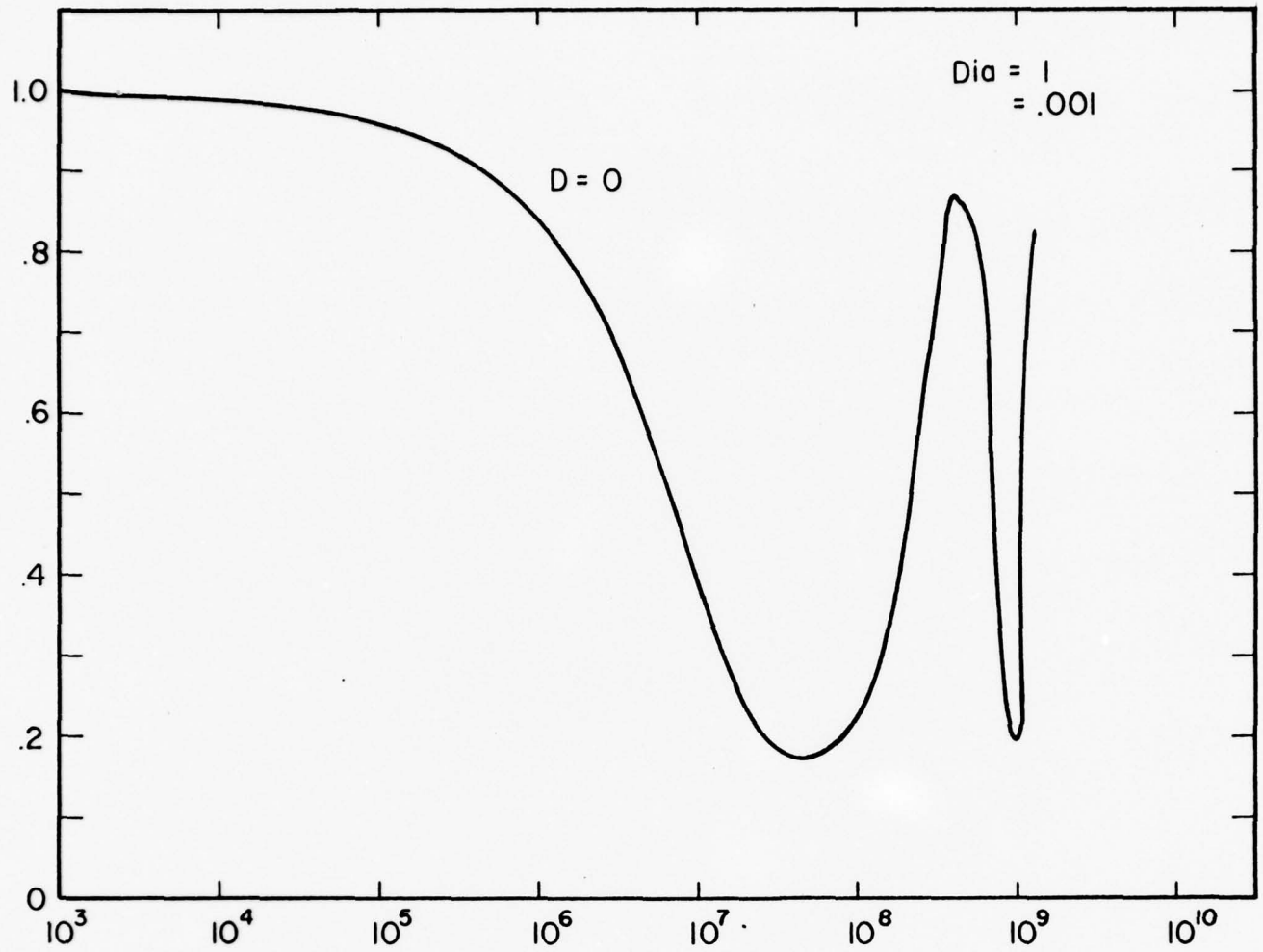

Figure 2 Steady State Transfer Function, diam = 2, $\sigma = 10^{-3}$ S/m, $\varepsilon_r = 7$, D = 0 m.

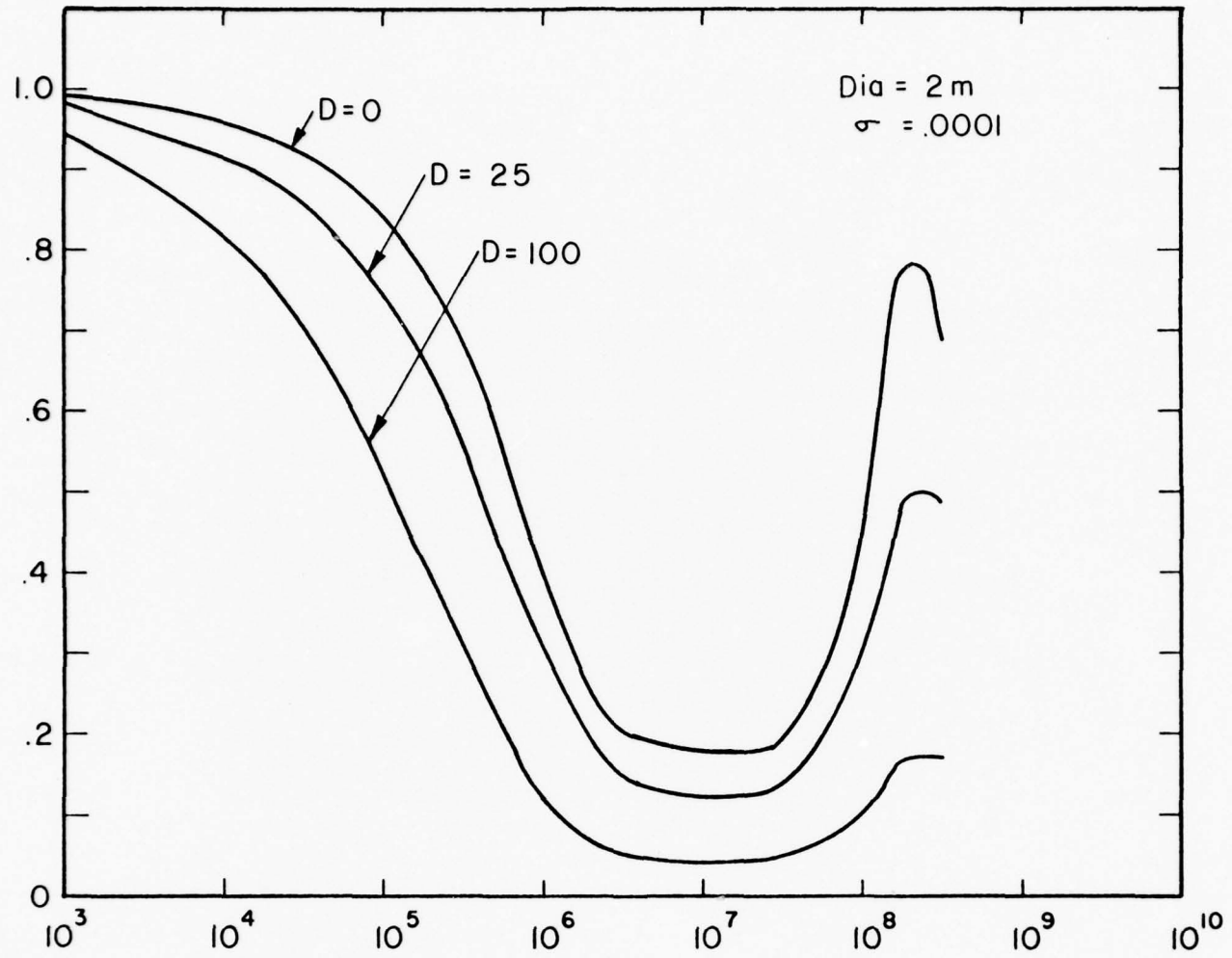

Figure 3 Steady State Transfer Function, diam = 2, $\sigma = 10^{-4}$ S/m, $\varepsilon_r = 7$, D = 0,25,100 m.

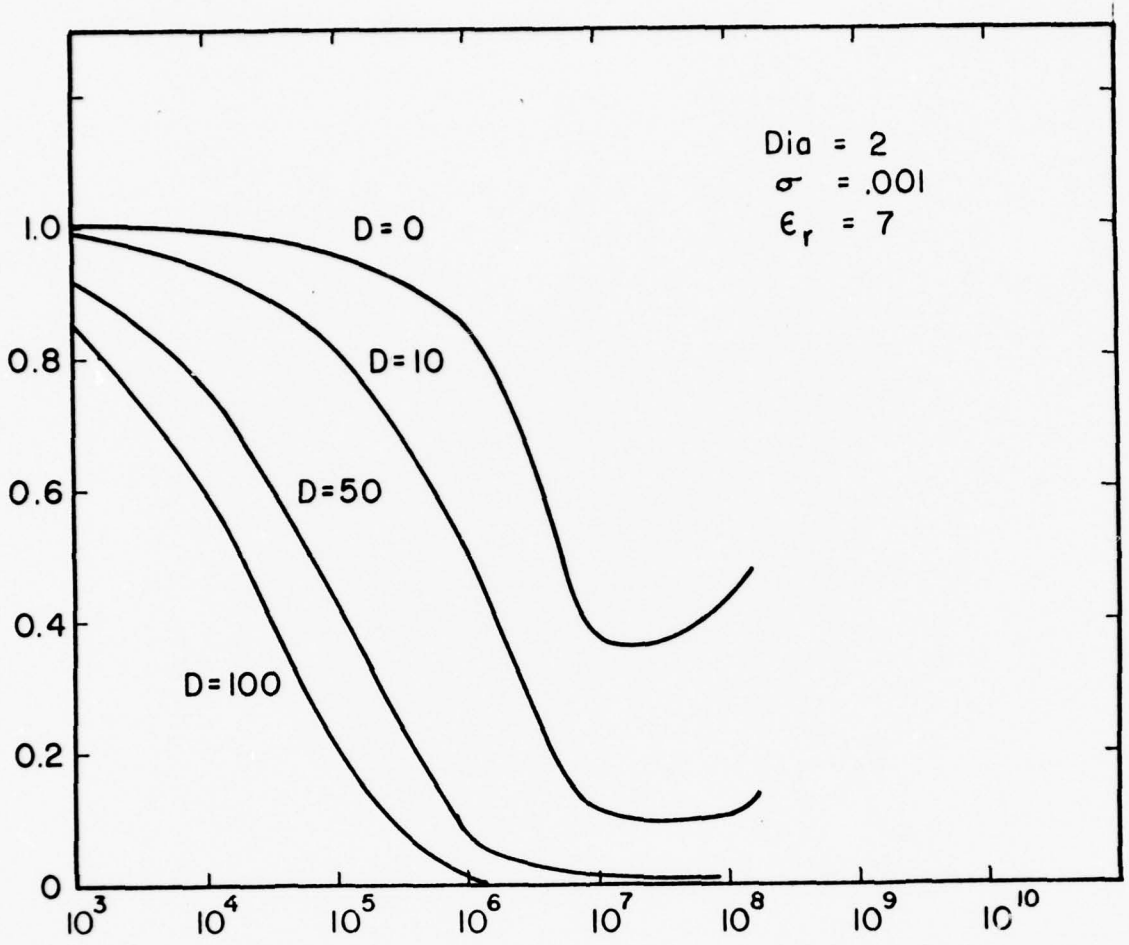

Figure 4 Steady State Transfer Function, diam = 2, $\sigma = 10^{-3}$ S/m, $\epsilon_r = 7$, D = 0,10,50,100 m.

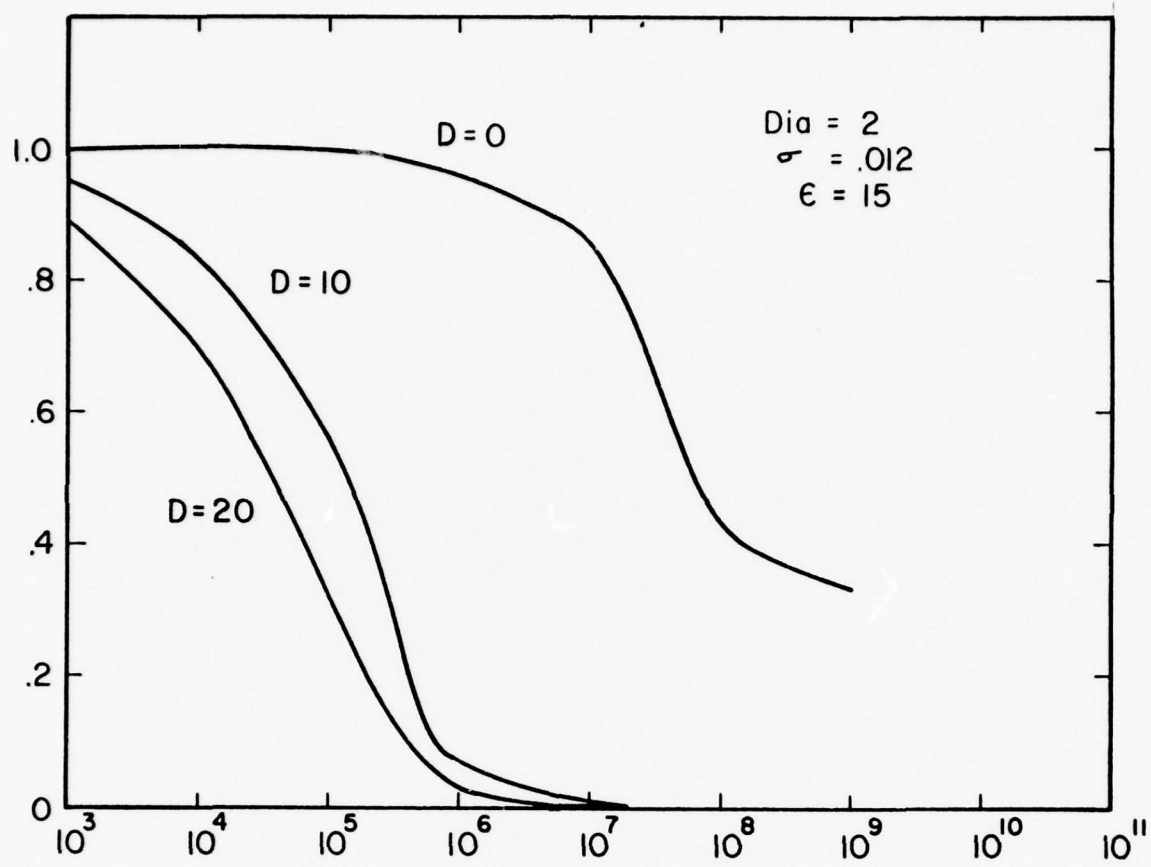

Figure 5 Steady State Transfer Function, diam = 2, $\sigma = 1.2 \times 10^{-3}$ S/m, $\epsilon_r = 15$, D = 0,10,20 m.

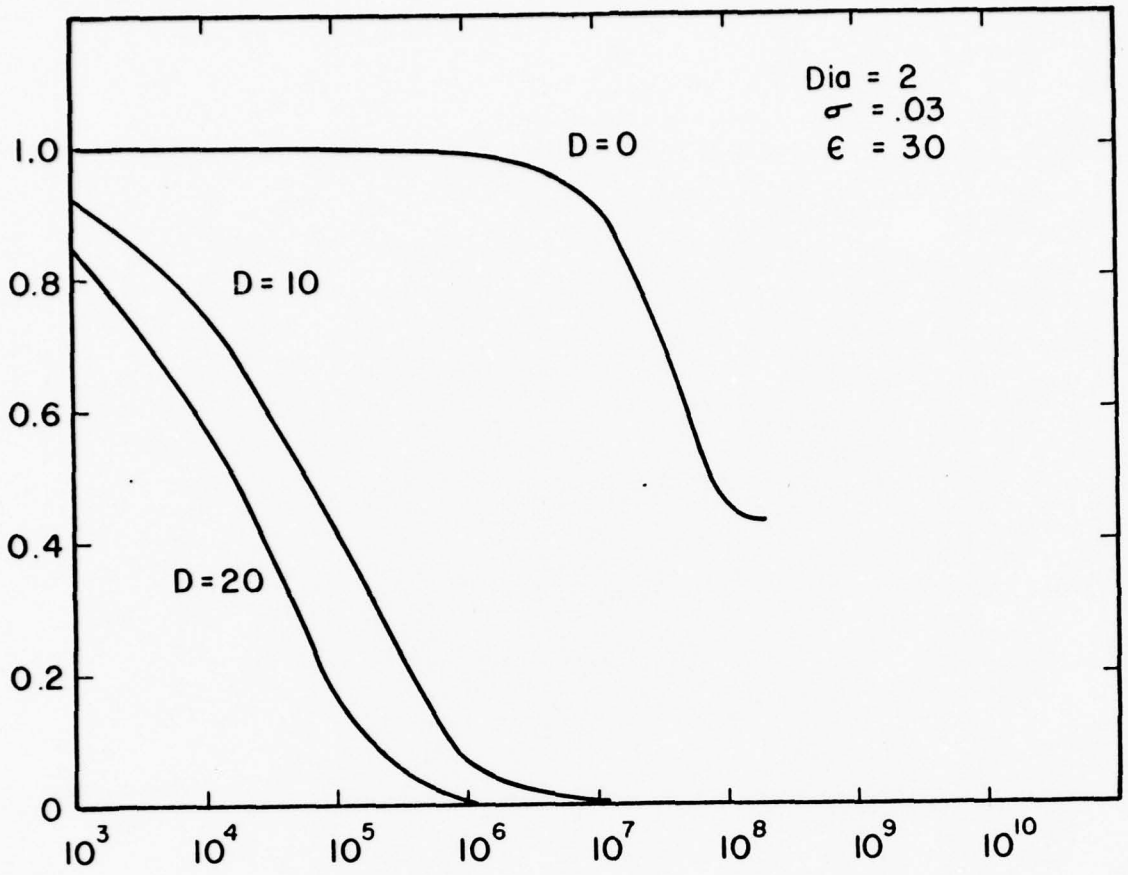

Figure 6 Steady State Transfer Function, diam = 2, $\sigma = 3 \times 10^{-2}$ S/m, $\epsilon_r = 30$, D = 0,10,20 m.

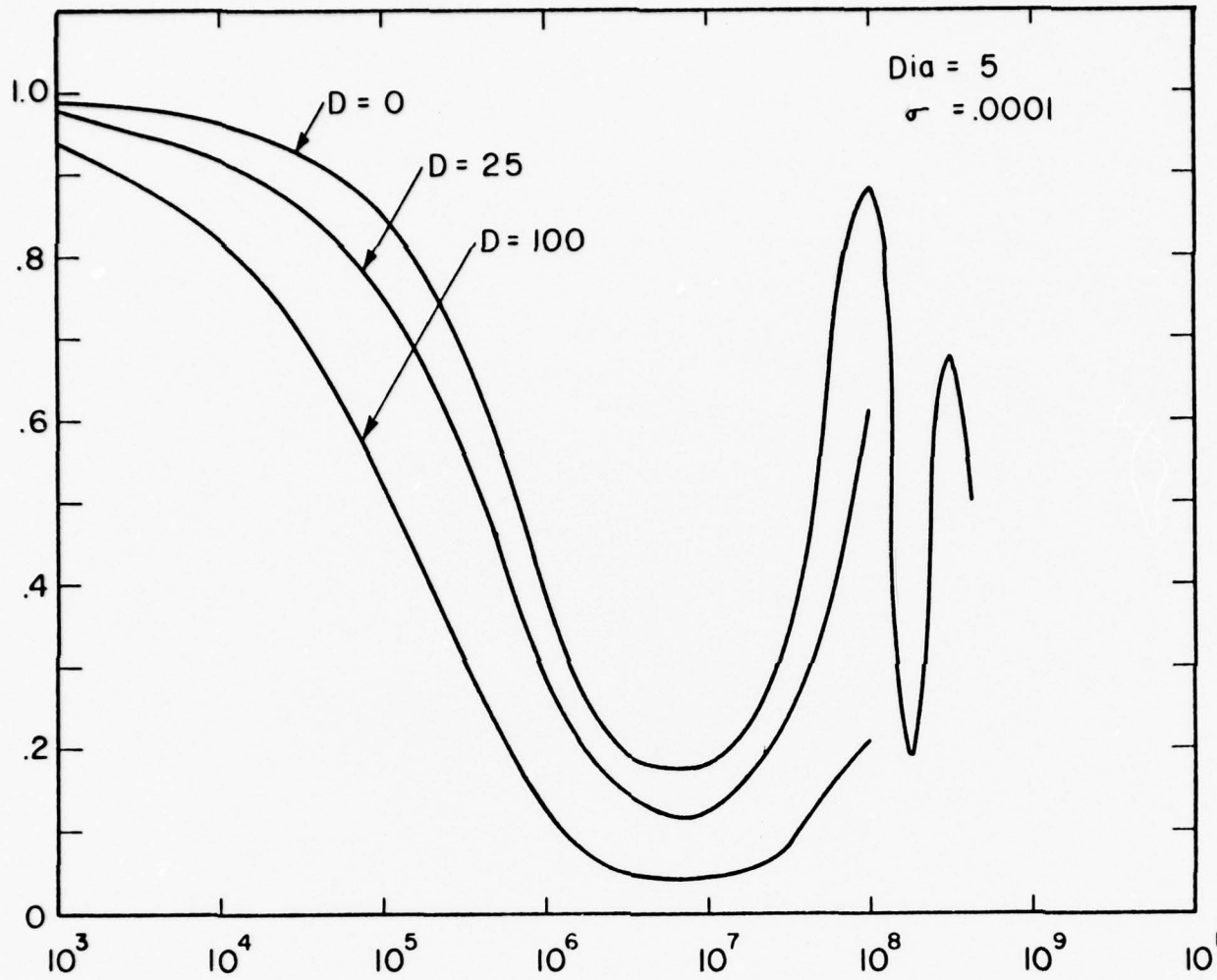

Figure 7 Steady State Transfer Function, diam = 5, $\sigma = 10^{-4}$ S/m, $\varepsilon_r = 7$, D = 0,25,100 m.

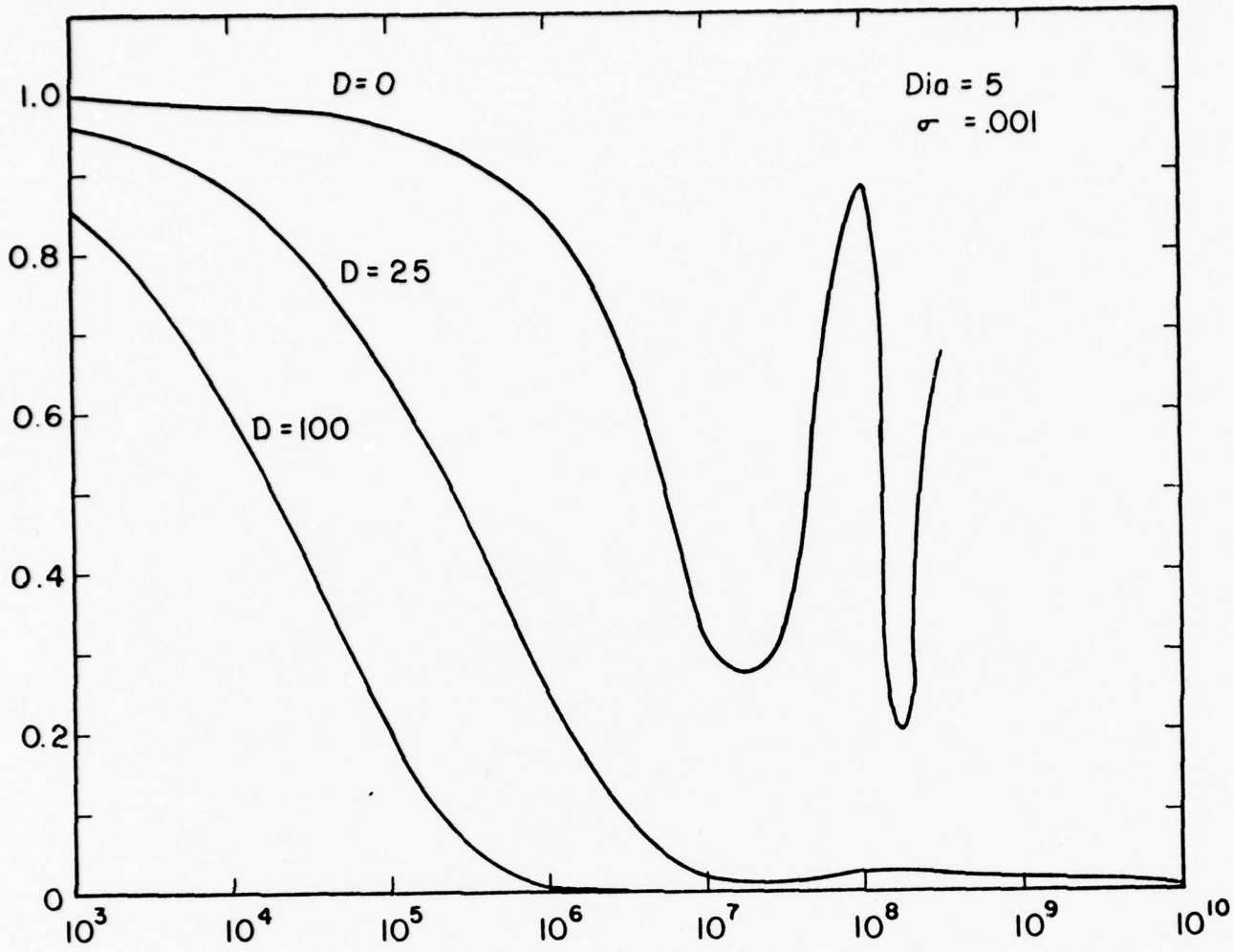

Figure 8 Steady State Transfer Function, diam = 5, $\sigma = 10^{-3}$ S/m, $\epsilon_r = 7$, D = 0,25,100 m.

B. Time Domain Pulses (t = pulse width)

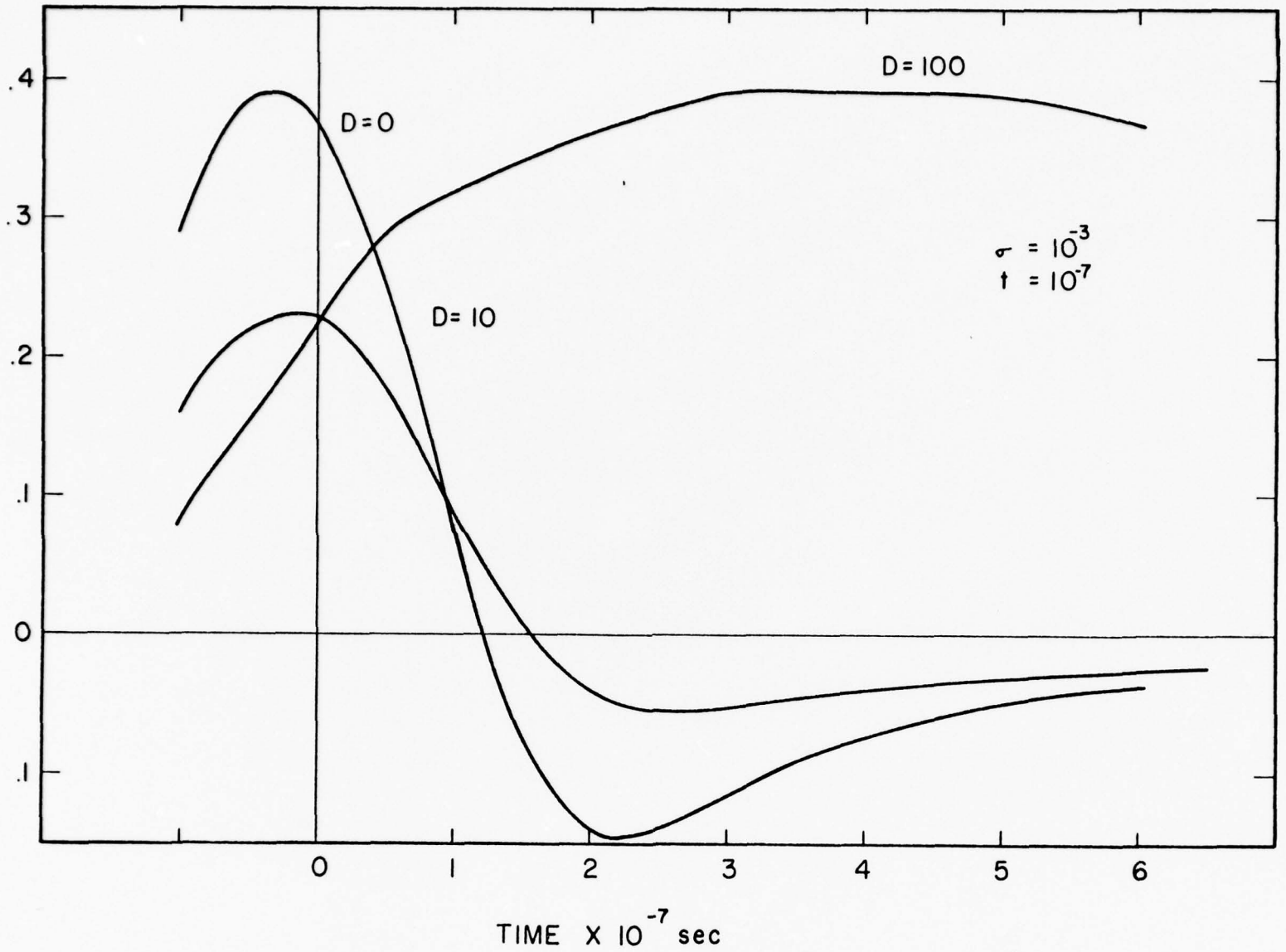

Figure 9 Gaussian Pulse from Air to Granite, t = 10^{-7} sec., σ = 10^{-3} S/m, D = 0,10,100 m.

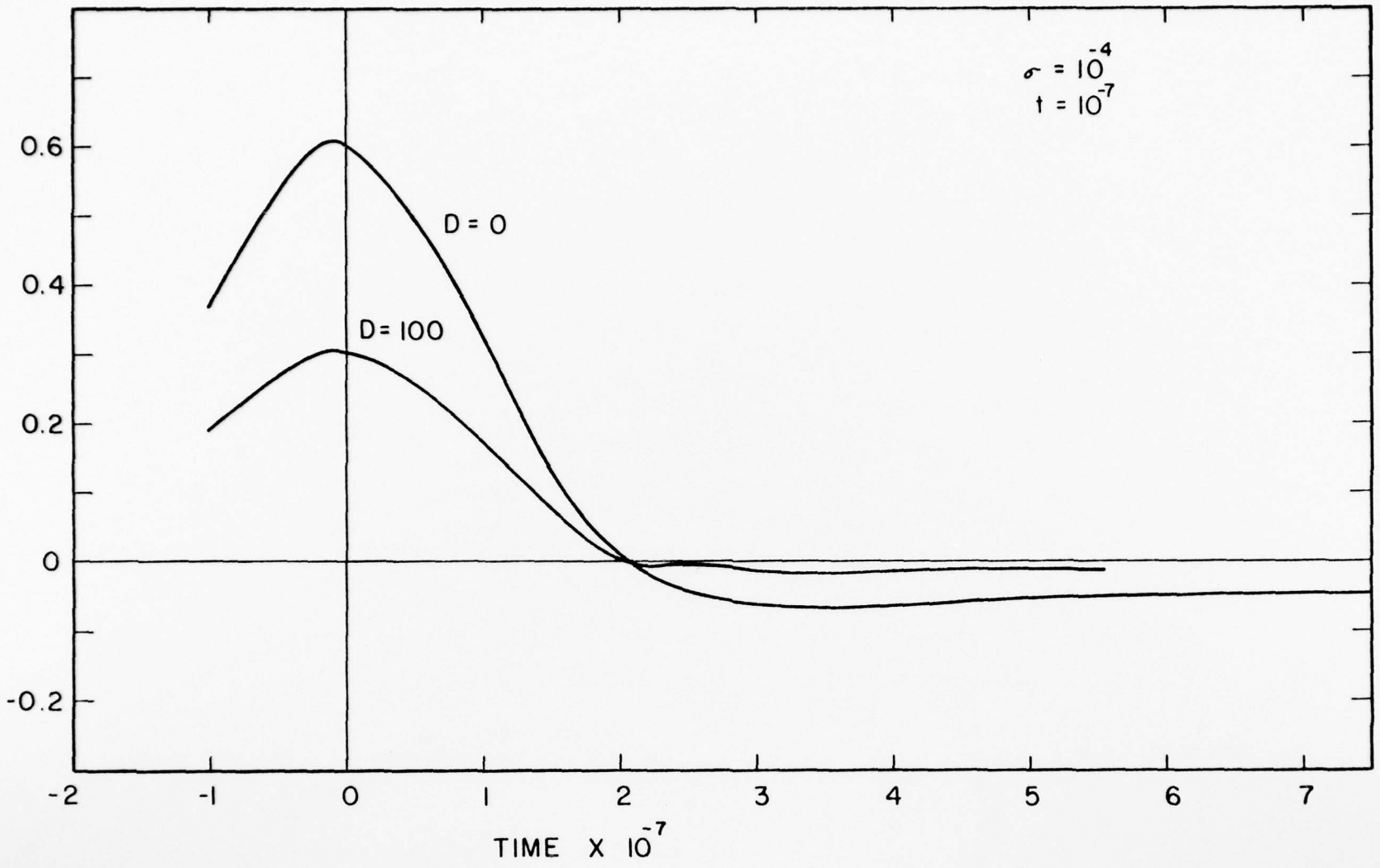

Figure 10 Gaussian Pulse from Air to Granite, $t = 10^{-7}$ sec., $\sigma = 10^{-4}$ S/m, D = 0,100 m.

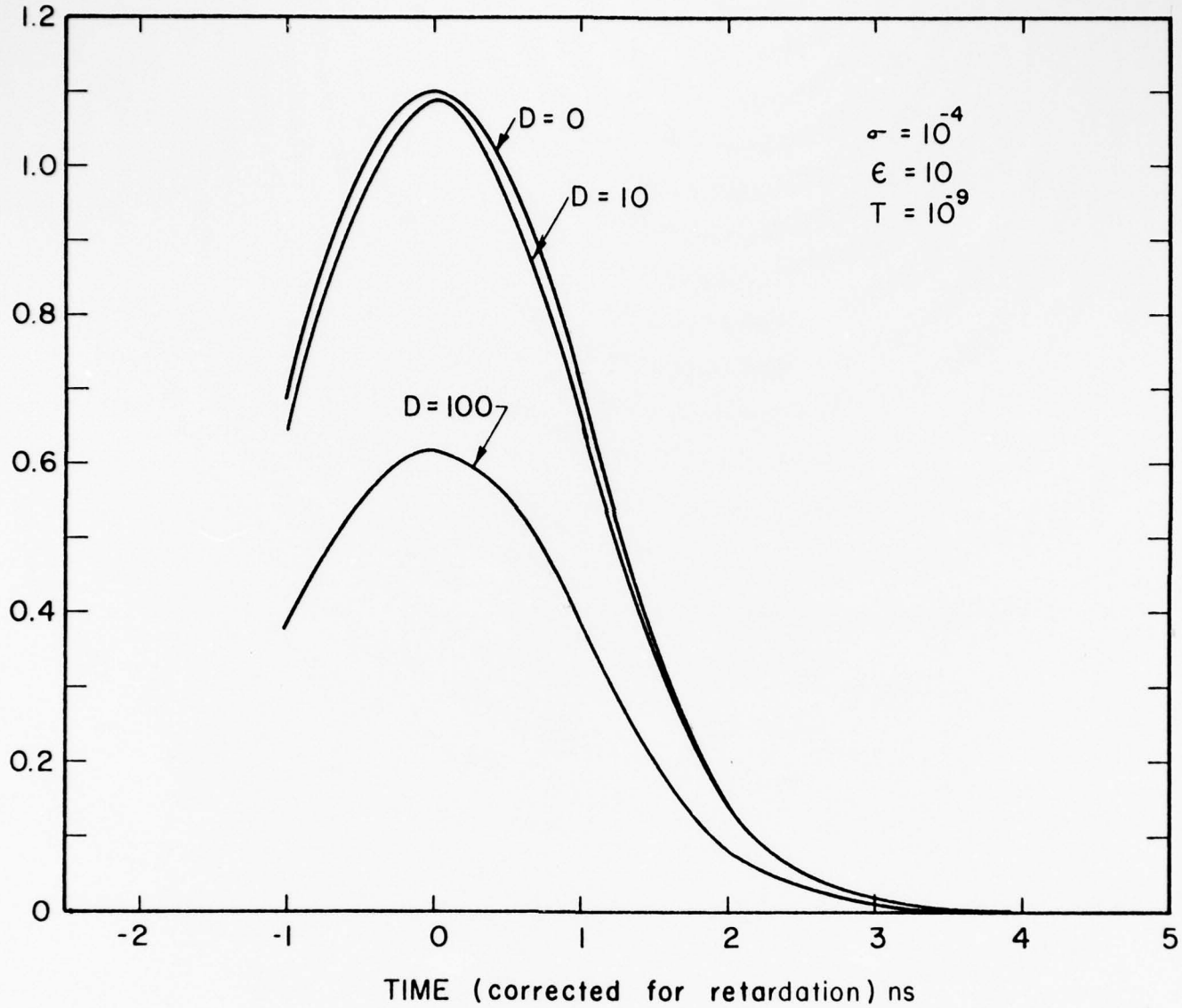

Figure 11 Gaussian Pulse in Granite at Different Depths, t = 10^{-9} sec., $\sigma = 10^{-4}$ S/m, $\varepsilon_r = 10$, D = 0,10,100 m.

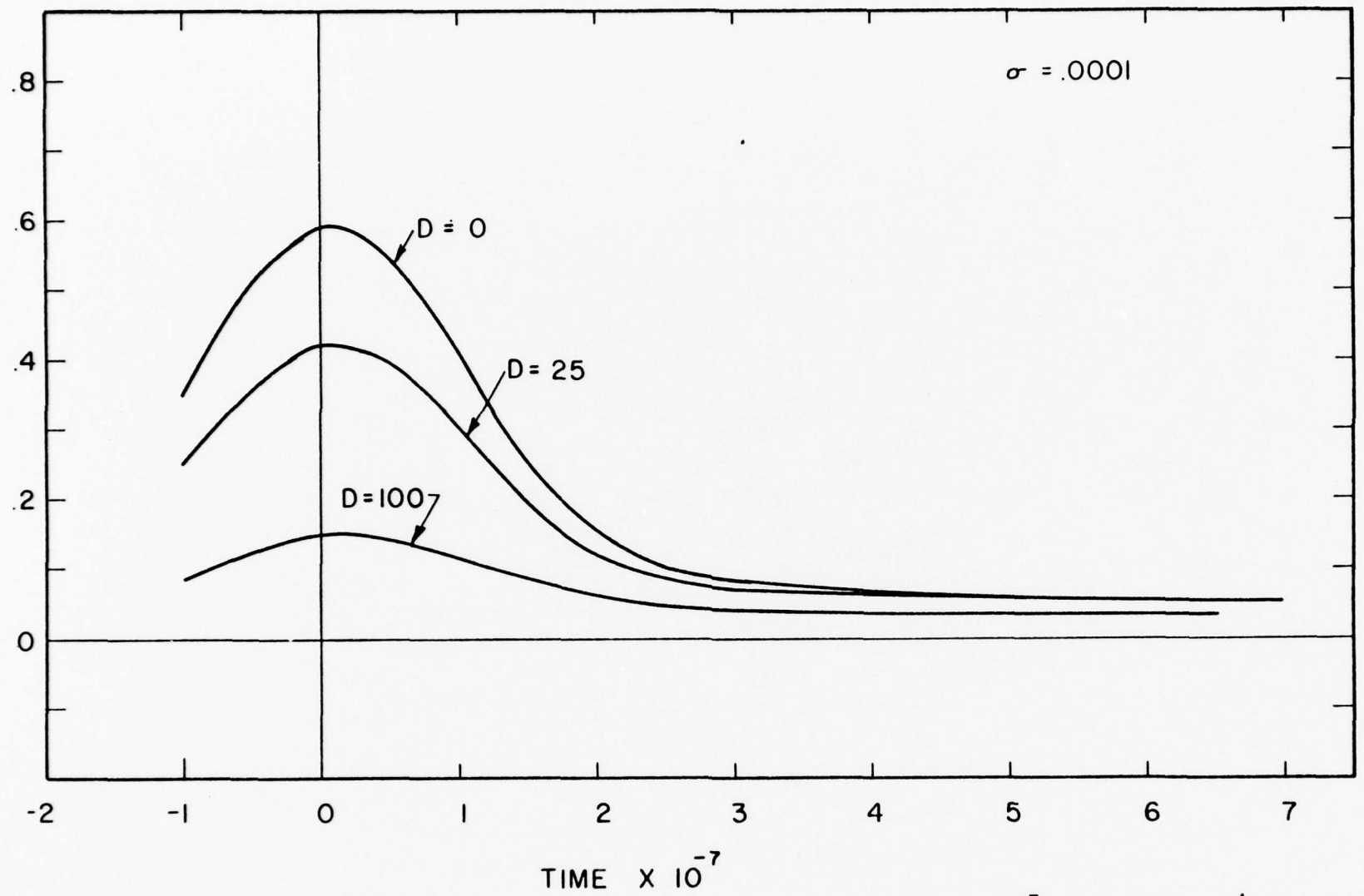

Figure 12 First Pulse into Tunnel for Different Diameters, t = 10^{-7} sec., $\sigma = 10^{-4}$ S/m, $\varepsilon_r = 7$, D = 0,25,100 m.

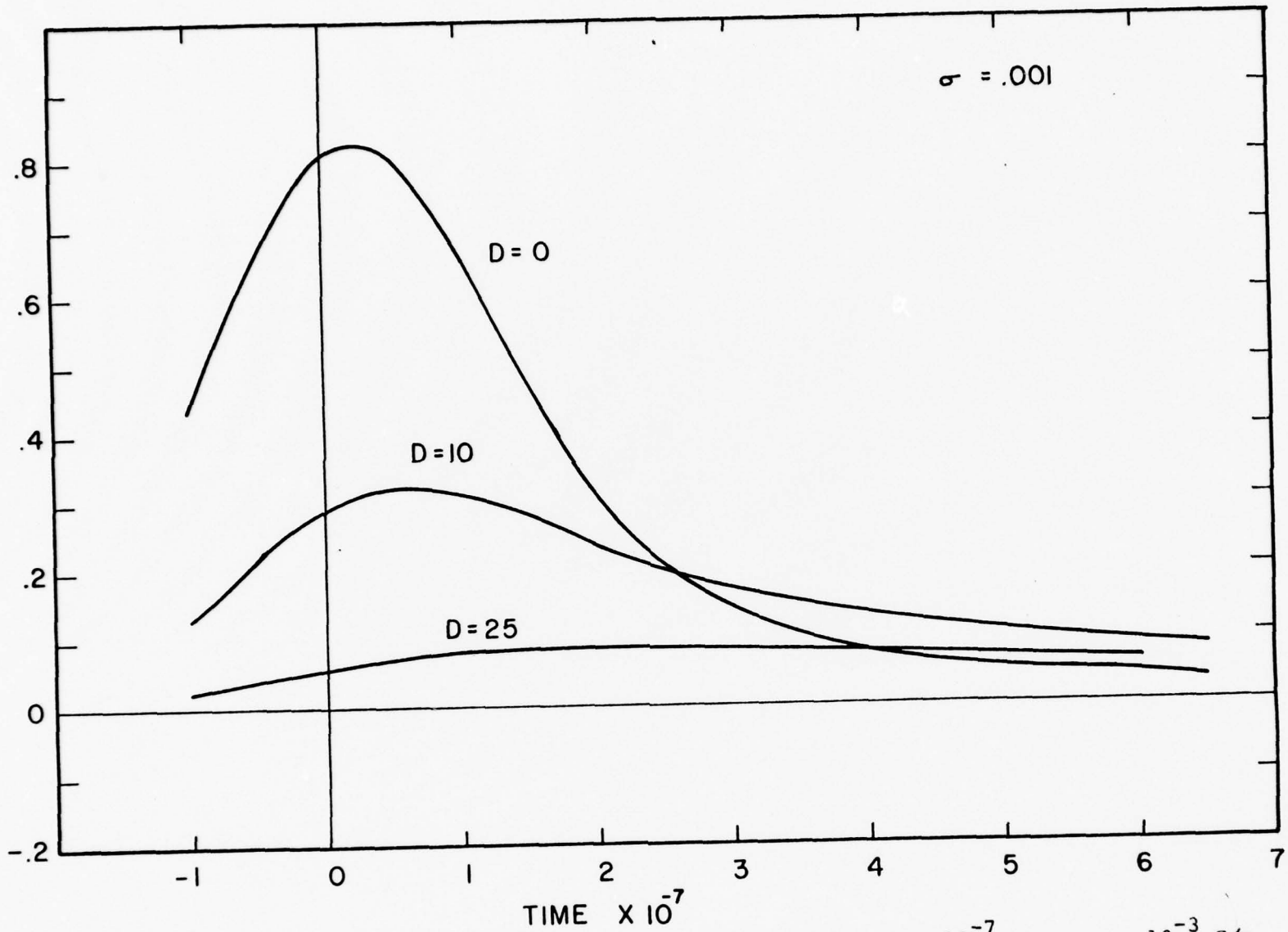

Figure 13 First Pulse into Tunnel for Different Diameters, $t = 10^{-7}$ sec., $\sigma = 10^{-3}$ S/m, $\varepsilon_r = 7$, D = 0,10,25 m.

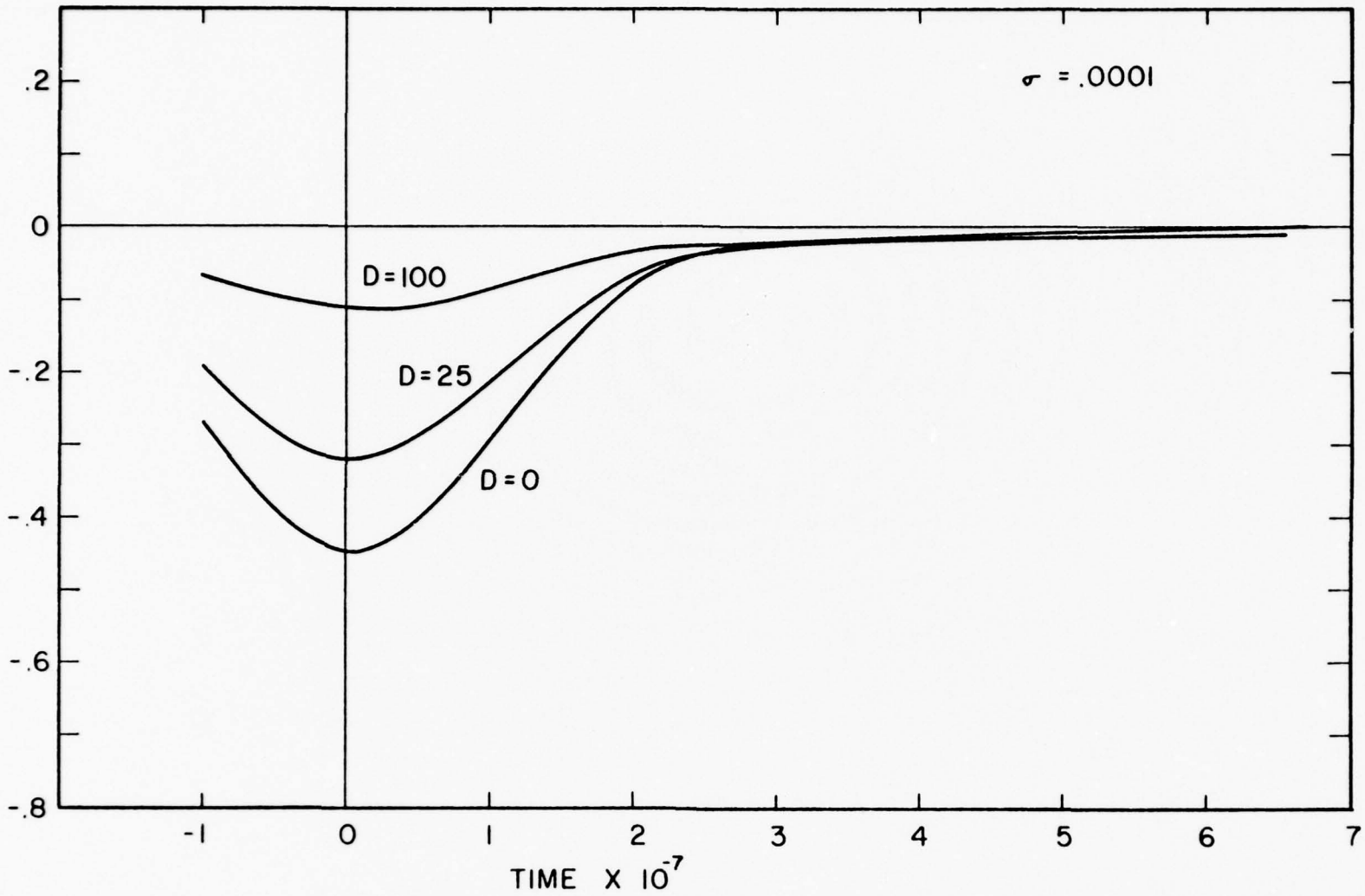

Figure 14 Second Tunnel Pulse from Bottom of Tunnel, t = 10^{-7} sec., $\sigma = 10^{-4}$ S/m, $\varepsilon_r = 7$, D = 0,25,100 m., diam = 2 m.

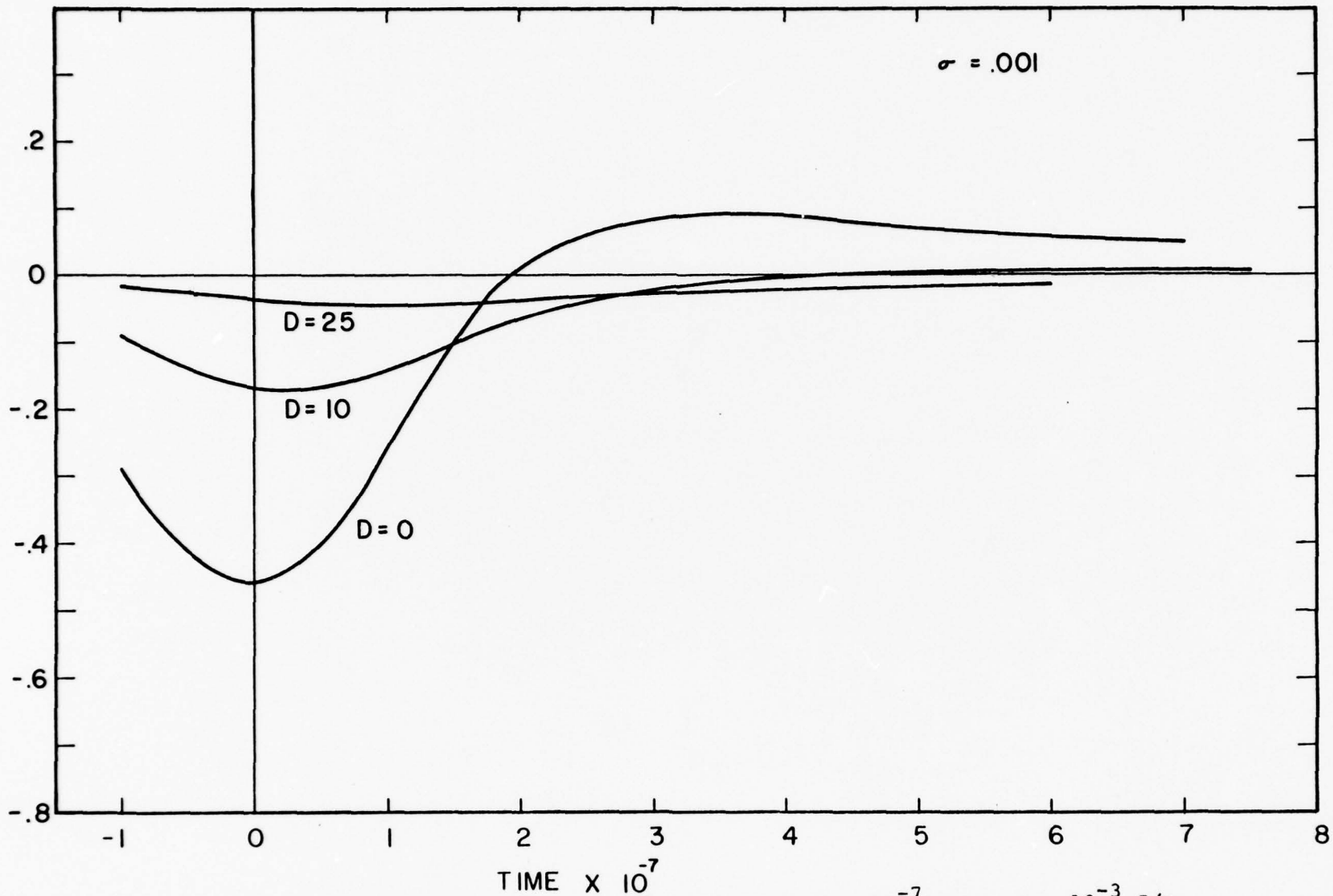

Figure 15 Second Tunnel Pulse from Bottom of Tunnel, t = 10^{-7} sec., $\sigma = 10^{-3}$ S/m, $\varepsilon_r = 7$, D = 0,25,100 m., diam. = 2 m.

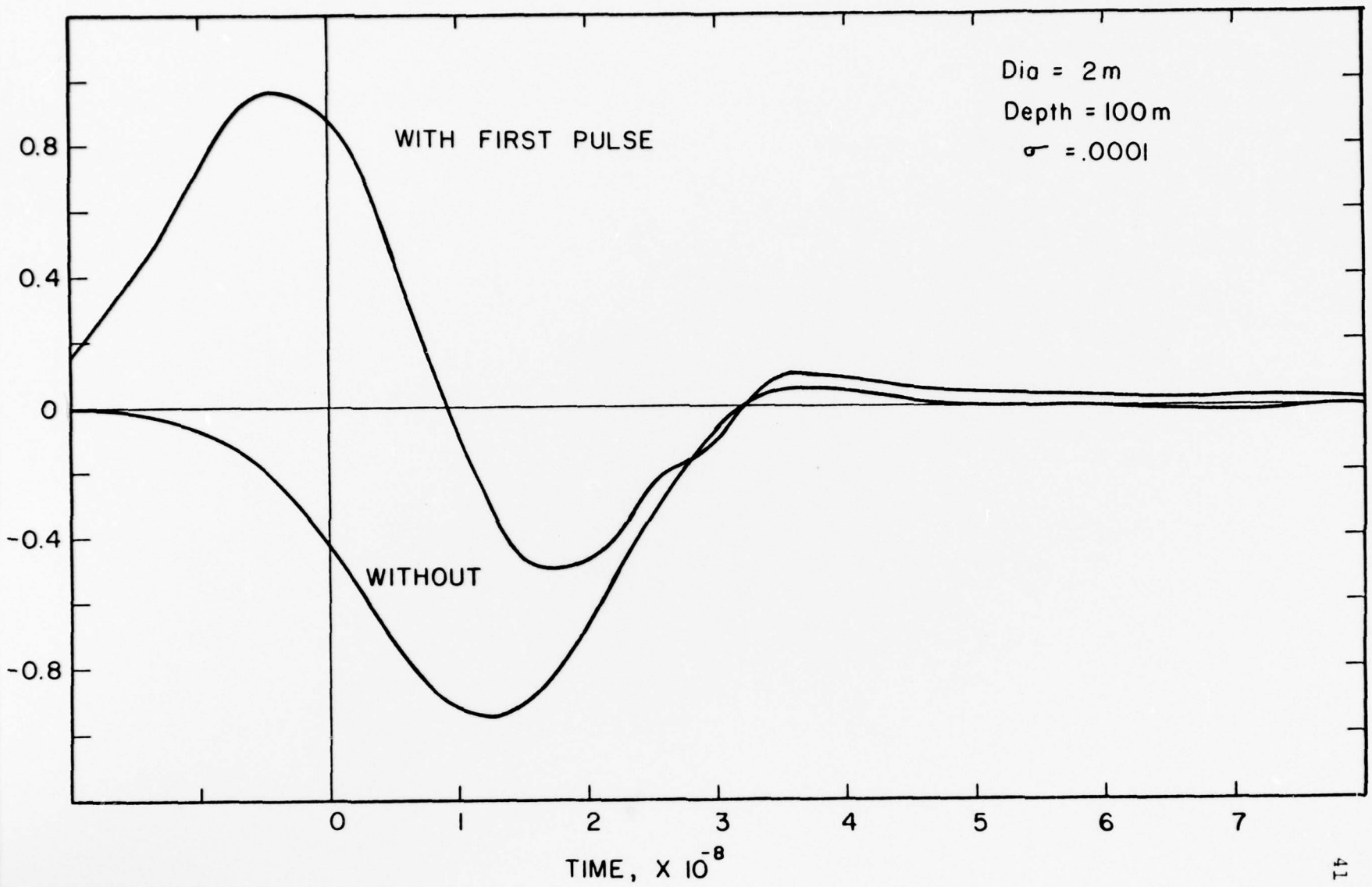

Figure 16 Pulse Returned from Tunnel With and Without First Reflection, diam = 2 m., D = 100 m., $\sigma = 10^{-4}$ S/m, $\varepsilon_r = 7$, $t = 10^{-8}$ sec.

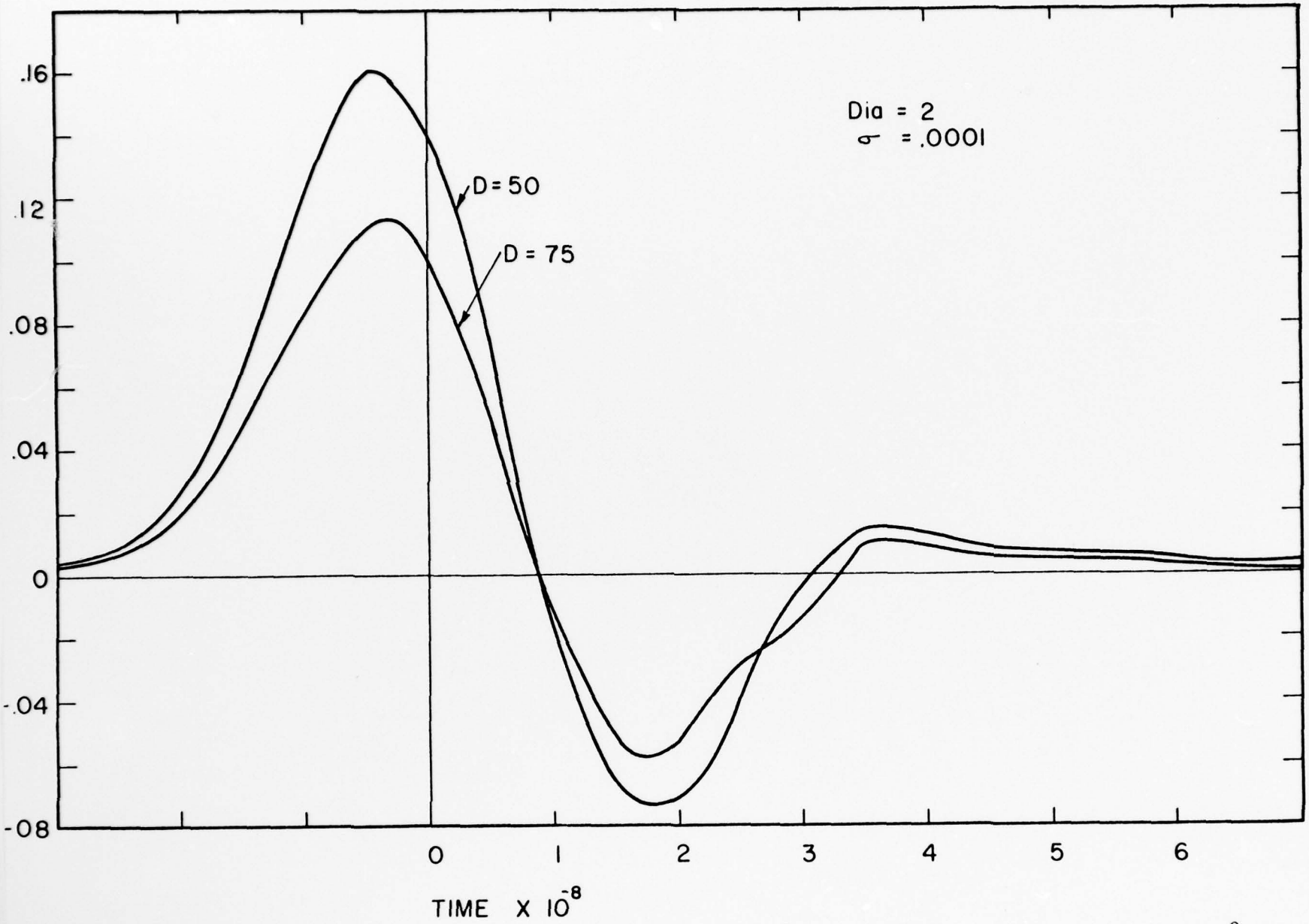

Figure 17 Full Tunnel Signal, diam = 2 m., $\sigma = 10^{-4}$ S/m, $\varepsilon_r = 7$, D = 50,75 m., t = 10^{-8} sec.

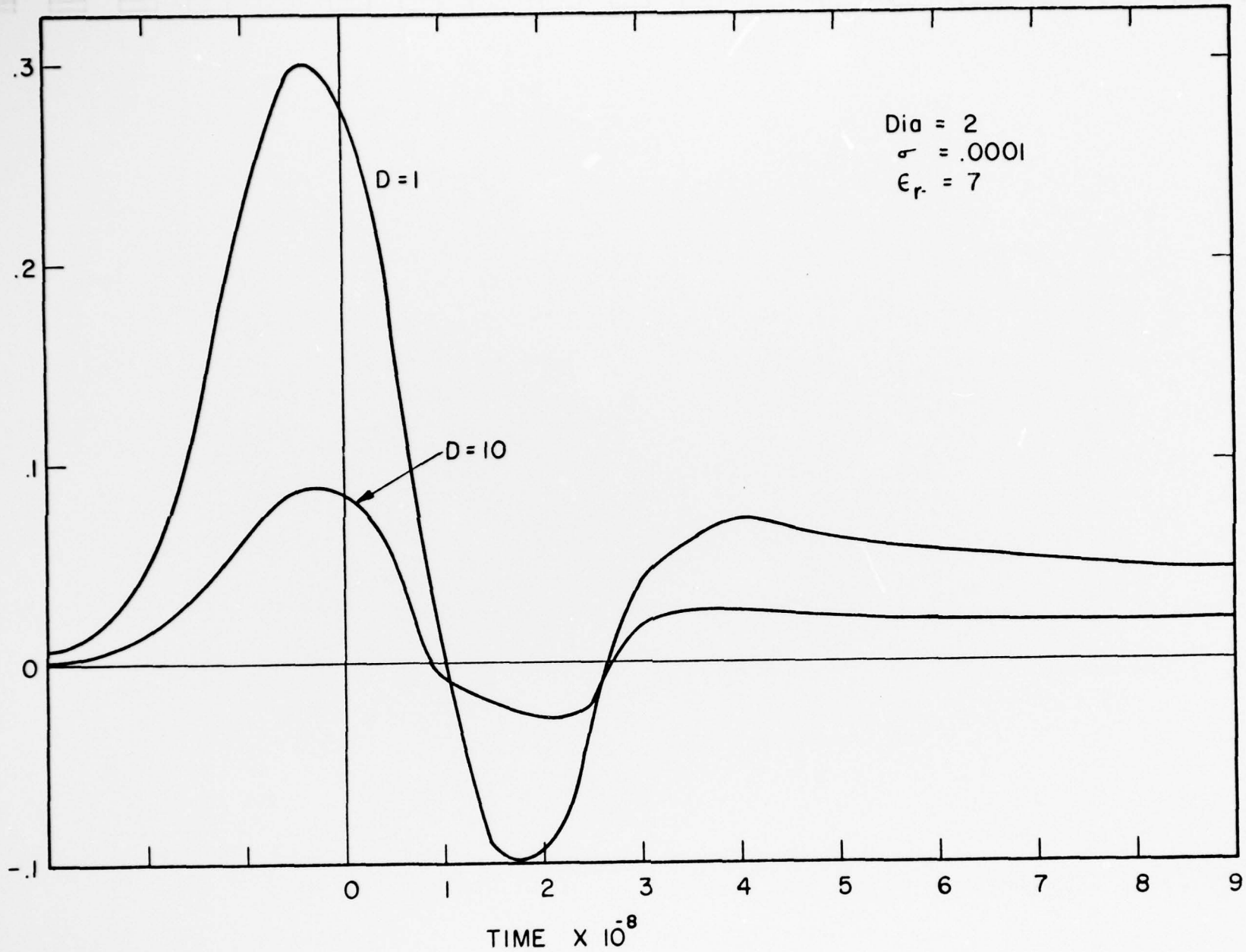

Figure 18 Full Tunnel Signal, diam = 2 m., $\sigma = 10^{-4}$ S/m, $\epsilon_r = 7$, D = 1,10 m., t = 10^{-8} sec.

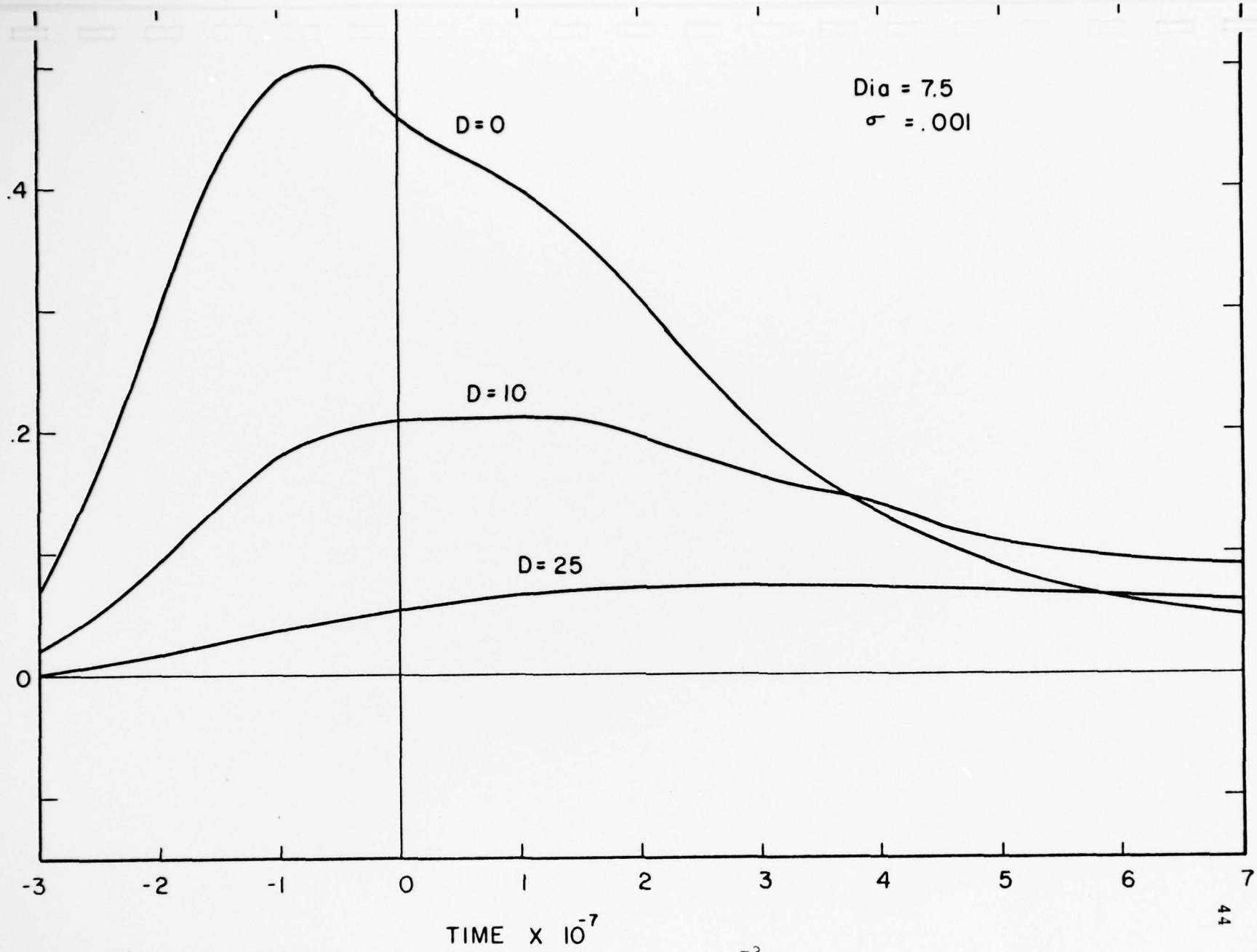

Figure 19 Full Tunnel Signal, diam = 7.5 m., $\sigma = 10^{-3}$ S/m, $\varepsilon_r = 7$, D = 0,10,25 m., $t = 10^{-7}$ sec.

III. Reconstruction of Arrays

The two programs which employed the reconstruction technique were BG;1 and BJS;1. The first BG;1 reconstructs an array from two projections, one vertical and the other at an angle ψ from the vertical. The other BJS;1 reconstructs from two projections at ψ from the vertical.

The first step in the reconstruction transforms the array (rectangular) into an area more convenient for the computation of the projections. In BG;1 the original rectangular array is transformed into a parallelogram (Figure 1). In BJS;1 the array is transformed into an array whose width is the same as the original array but whose length is chosen to fit as closely as possible to the original length. Every other point in this array is not part of the grid (Figure 2).

The positions of the new points are computed and corresponding densities are found by using a Cardinal Series Interpolation technique. That is, the contribution to the new density from an old density point is given by $\frac{\sin a\pi}{a\pi} \cdot \frac{\sin b\pi}{b\pi}$ where a and b are the x and y distances between the points. The sum is over the nearest 16 points.

The appropriate projections (P,Q) from these new densities are required. The first order approximation to the reconstructed array is set out in such a way that the Q projections are satisfied. New P projections are computed and all points in a

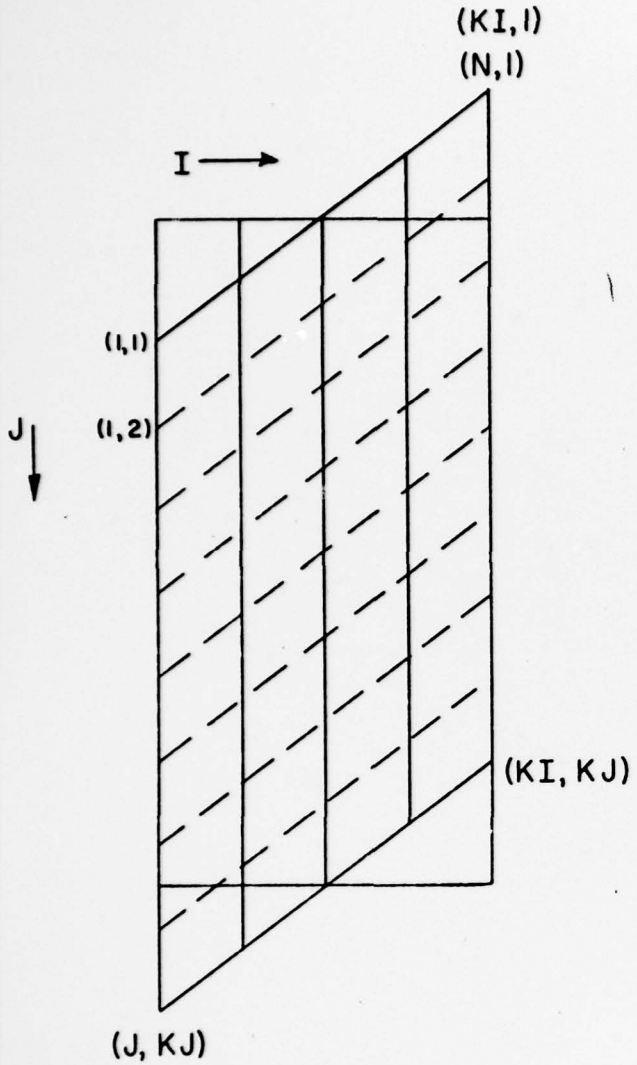

Figure 1 Rectangular Array Transformed into a Parallelogram

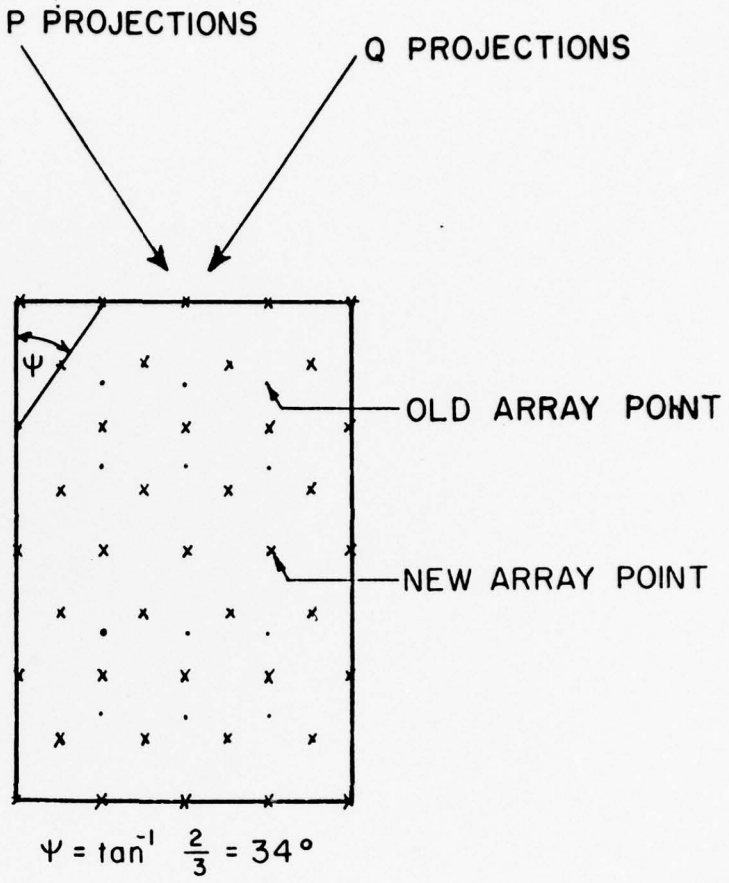

Figure 2 Transformation of Array Points

given P row are scaled by a constant factor so as to satisfy the original P projections. Then the same is done for the Q projections. This iterative process is applied until both projections are satisfied to the desired degree of accuracy. This usually takes fewer than four sets of iterations.

In BJS;1 the possible tunnels are located by first smoothing both P and Q projections (P(J) = (P(J-1) + 4P(J) + P(J+1)/6) and then looking at the intersections of the maxima of P and Q. Where a point determined by the intersection of two of these projections is found to be within the array, an average over the nearest four points is taken and output along with the coordinates of the possible tunnel. These sums are an indication of the "strength" of the tunnel. Figure 3 shows the array geometry and Figure 4 the projection sums.

The width of the projection maxima are an indication of the size of the tunnel, and finer detail in the "skirts" of the array will help distinguish tunnels from other possible targets.

IV. Reflection and Propagation of Pulses

Several programs were written to study the propagation of electromagnetic pulses through granite (and other materials) and the reflection and transmission of these pulses from various granite-air interfaces. The final program TT.FOR;2 gives the electric field intensity at the surface (as a function of time) from a Gaussian wave which travels a distance D through granite,

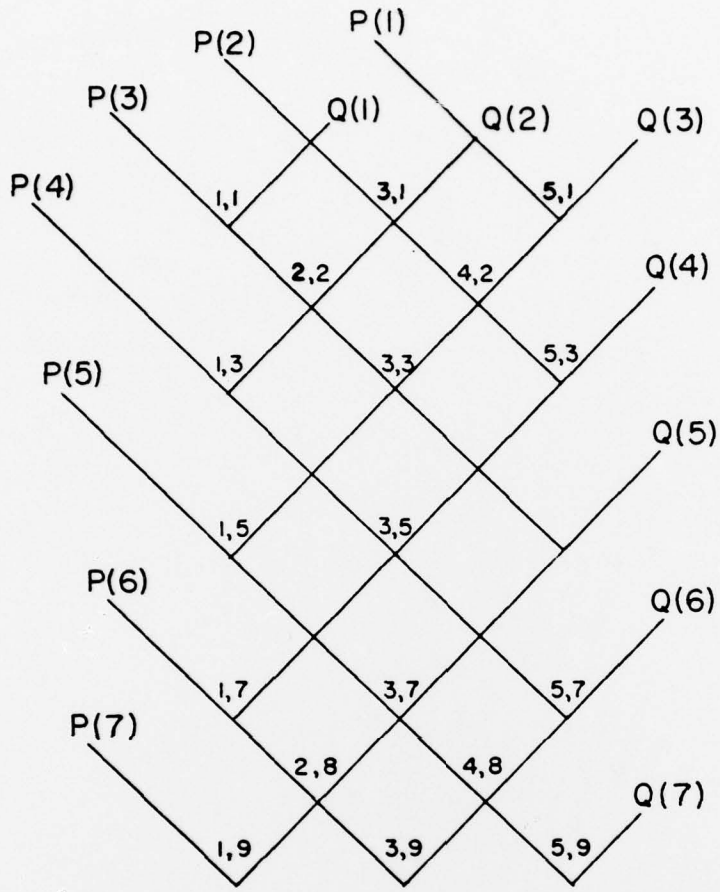

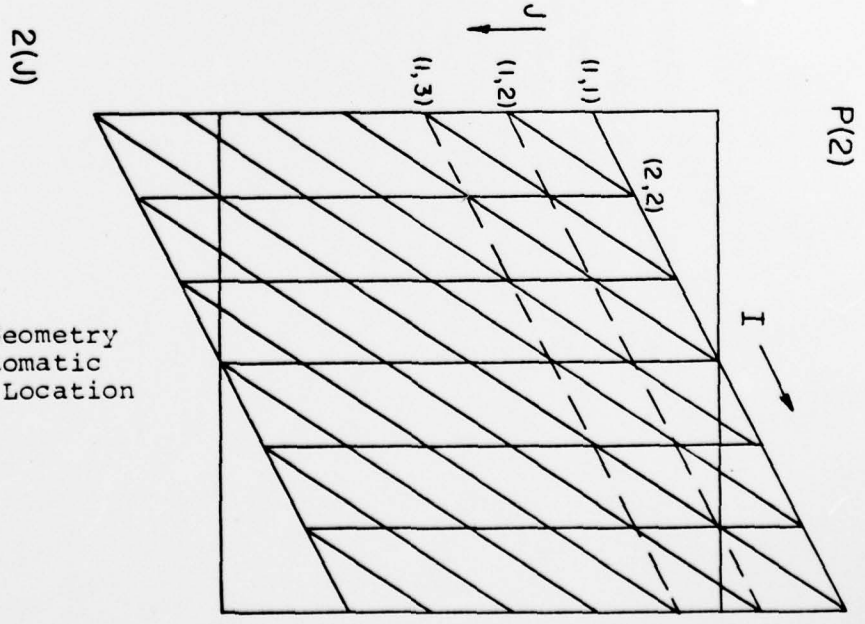

Figure 3 Array Geometry for Automatic Target Location Scheme

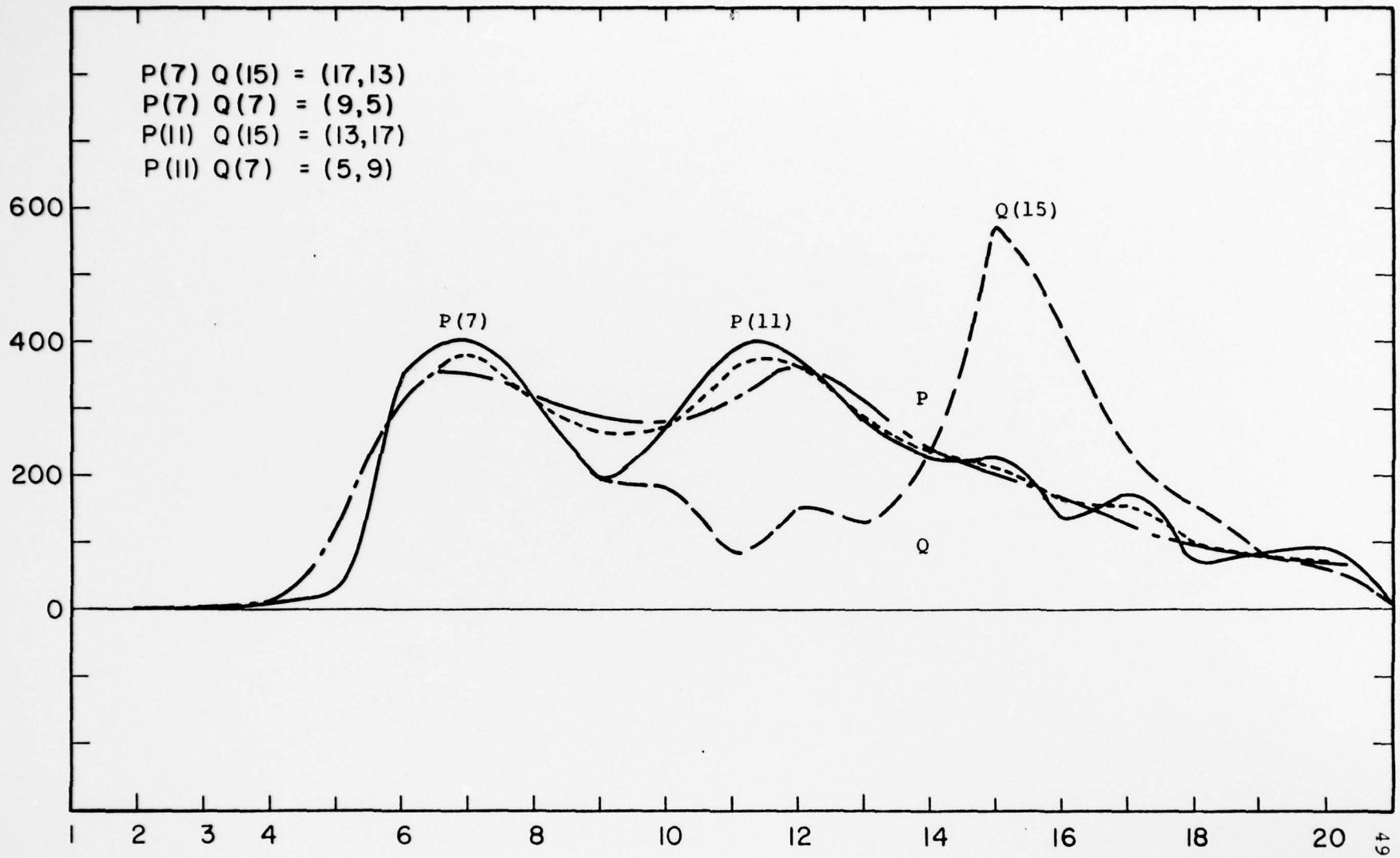

Figure 4 Projection Sums for Automatic Target Location Scheme

is then reflected (three times) from an air filled cylinder and finally propagates back to the surface.

The computations were done in the frequency domain. A steady state transfer function was computed and Fourier transformed back to give a real time domain signal. The integral involved required from 100-400 iterations to converge. The limits of the integral are from $\omega = 10^4$ to $\omega = 2.6/T1$. For lower frequencies the transfer function was nearly constant so the contribution to the integral was neglible. For frequencies higher than 2.6/T1 the Gaussian envelope sends the integral to zero. The ω integral used unequal spacing since the transfer functions decreased exponential with ω. This gave nearby equal intervals areas for each $\Delta\omega$. (i.e., as many points were used between $\omega = 10^7$ and 10^8 as between $\omega = 10^6$ and 10^7, etc.)

Another program computes the transmitted pulse (air→granite) to a depth in granite to compare with work done by others. The resultant pulse agreed exactly with the work done by King and Harrison.

Programs which output the transfer functions (magnitude vs frequency) were also written to investigate the relationship between tunnel size, pulse width and particular electrical characteristics of the granite.

The final program G1.FOR;1 created an array of "density" points resembling a real electromagnetic subsurface profile. The return pulses to a point sweeping across the earths surface (perpendicular to the tunnel) were transformed to corresponding depth positions and output on a grid. For most of these investigations the following parameters were used: $\varepsilon_r = 7, \sigma = 10^{-3}$ or 10^{-4}, pulse width 10^{-7}, 10^{-8}, or 10^{-9}.

V. Program Descriptions

BJS;1 — The reflected pulse array (9,43) is read from disk, (FOR20.DAT, the latest version is read). The computer then asks for a projection angle PHI(I2). It then creates an array whose size most nearly fits the original array such that the projections from points A(N,M) to A(N+1, M+1) or A(N-1, M-1) are at the angle ±PHI.

New densities at these points are formed from the old densities by using a Cardinal Series Interpolation formula for the sixteen points nearest the new density point. Projections (P,Q) at an angle ψ from the vertical are then computed and a zeroth order approximation satisfying the Q projections. P and Q projections are then alternately satisfied until the array converges.

The program outputs the projections, the reconstructed array, possible tunnel positions and then a gray scale equivalent of the array. The tunnels are found by first smoothing the P and Q projections and then looking at the intersections of their respective maxima, 1.

After the gray scale is output the machine waits for a -1 or 1 input (I2). A -1 ends the program and a 1 will make the program ask for a new input angle.

BJS;2 — OUTPUTS A GRAY SCALE WITH 10 shades.

BI;1 — Same as BJS;1 but does not involve reading the array from the disk, or output the tunnel location. It asks for the I and J dimensions and then for the array. I and J must be odd.

BG;1 — Reads a (9 x 30) array from the disk (FOR20.DAT), transforms the array to an array in the shape of a parallelogram and then proceeds like BJS;1 except the two projections are vertical and at an angle ψ. The output is the projections, densities and gray scale.

After the projections are output the machine waits for an IZ input. If IZ=0 the iteration is done two more times. If IZ=1 is outputs the gray scale and the array, if IZ=2 it goes back for a new angle and if IZ=3 it ends.

BE;1 — Same as BG but does not read from the disk and also outputs the original new densities

G1.FOR;1 — An array is outputed which corresponds to a scan across the earth's surface from -60 to 60 meters. The output is the array positioned relative to the earth as it would appear on an ESP. The seventh output now corresponds to the position of the return peak from the x=0 reflected pulse. Each subsequent row is at a time increment of half the pulse width.

The input format is:
DEPTH - distance to the top of the cylinder, F5.1
ITERATIONS - number of iterations in the integral, I3
SIGMA - effective conductivity, F6.5
TIME - pulse width, E5.0
DIAM - diameter of the cylinder, I1
SCALE - scale factor for output, I2
IW - switch to include first pulse IW=1 or leave it out IW=0, I1

G2.FOR;1 — Same as G1.FOR;1 but X goes from -40 to 40 and there is an option to also output (IW=1) the combined signal from two other tunnels located at X = -20 and +20 with diameters of 0 and 6. (This does not work correctly because of how TT is used). Note: IW is not the same as in G1.FOR;1.

G.FOR;1 — Outputs array grid without the earth spacing as in G1.FOR;1.

TT.FOR;2 — The time domain reflected pulse from a cylinder embedded in granite. The seventh output point corresponds to the peak of the pulse. The integral for each value of the time is performed by taking increments of w which are exponential.

The input format is:
DEPTH - I3 - depth to top of cylinder
ITERATIONS - I3 - number of iterations in the integral (greater than 100)
SIGMA - F6.5 - effective condictivity
TIME - E5.0 - pulse width
DIAMETER - I1 - diameter of cylinder

T.FOR;5 — Same as TT.FOR;2 but computes the integral from $w = 10^6$ instead of 10^4 and uses 1/2 the value of the first point. (Output varies considerably from TT.FOR;2).

TT.FOR;1 — Same as TT.FOR;2 but without first pulse.

T1.FOR;2 — Same as TT.FOR;2 but outputs 100 points from T=0 to T=200T1

TS.FOR;1 — TT.FOR;2 but outputs the value of the integral in the summing loop at T = the center of the pulse position.

TS.FOR;2 — TS.FOR;1 but outputs the function for $w = 12 \times 10^8$ at T = center of pulse. For T different from this, the output is markedly different.

U.FOR;1 — Similar to TT.FOR;1 but computes the pulse as the sum of three separate transfer functions. Also, the cylinder diameter is adjusted to the nearest T1/2 interval of delay time. (Phase difference, in time, for each of the three pulses is always a multiple of T1/2).

AC;1 — Reconstruction of an odd square array for an angle from the vertical and the vertical.

BC;1 — Reconstruction on an NxM odd array as in AC1;.

H.FOR;1 — Computes the transfer function for reflection from a cylinder using first three reflected pulses. W goes from 10^3 to 10^{10}, 15 points are output.

Input format is:
DISTANCE - depth to cylinder, F5.1

SIGMA - effective conductivity, F6.5
DIAMETER - diameter of cylinder, I2

HH.FOR;1 — Same as H.FOR;1 but W goes from 2.6×10^8 to 10^9 with 55 points output.

HH.FOR;2 — Same as H.FOR;1, but W goes from 10^9 to 10^{10} with 35 points output.

RAN1;1 — Reads a 9 x 43 array FOR22.DAT adds a random number to each element and writes the result on FOR20.DAT. The average random number is half the maximum.

Input:
MAX RAN NUMBER - I3

GR1;1 — Reads FOR20.DAT (9 x 43) and outputs gray scale on TTY. 6 shades are used, 0,1,2,3,4,5.

T.FOR;1 — Outputs cylinder reflection from first two reflected pulses using two transfer functions. The two pulses are output separately, not the sum. The cylinder has zero diameter.

S.FOR;1 — Reflected pulse going from granite to air, through D meters of granite.

S1.FOR;1 — Output 50 points for S.FOR;1; T = 4T2 200 T1

R.FOR;1 — Transmitted pulse from air-granite to depth D.

X.FOR;1 — Transfer function for free pulse in granite multi-optical by Gaussian envelope $\exp(-\omega^2 t^2/2)$.

Q.FOR;1 — Transmission of free pulse in granite $\sigma = 10^{-4}$, $t = 10^{-9}$ sec.

P.FOR;1

C.FOR — Plots reflection from sphere.

A. Data Files

FOR21.DAT;1 — 9 x 3 array of one pulse from -40 to 40 meters.

FOR21.DAT;3 — 9 x 43 array of two pulses from -40 to 40 meters.

FOR21.DAT;2 — 9 x 43 array of one pulse.

FOR21.DAT;4 — 9 x 43 array of one pulse with blotch and stripe.

References

1. Kouyoumjian, R. G., Peters, Jr., L., and Thomas, D. T., "A Modified Geometrical Optics Method for Scattering by Dielectric Bodies," I.E.E.E. Transactions on Ant. and Prop. November 1963, pp. 690-703.

2. Sandler, S. S., "Picture Processing and Reconstruction," Lexington Books (Division of D. C. Health) 1975, see Chapter V.

3. King, R. W. P. and Harrison, C. W., Jr., "The Transmission of Electromagnetic Waves and Pulses into the Earth," J. App. Phys., Vol. 39, No. 9, 4444-4452, August 1968.